

REPORT DOCUMENTATION PAGE

AFRL-SR-AR-TR-05-

Public reporting burden for this collection of information is estimated to average 1 hour per response, including the time for reviewing the data needed, and completing and reviewing this collection of information. Send comments regarding this burden estimate or any reducing this burden to Washington Headquarters Services, Directorate for Information Operations and Reports, 1215 Jefferson Davis Highway, Suite 1204, Arlington, VA 22202-4302, between 12 p.m., January 1, 2002 and 12 p.m., December 12, 2002.

| | | | |
|---|--|--|----------------------------|
| 1. AGENCY USE ONLY (Leave blank) | 2. REPORT DATE 4-15-2005 | 3. REPORT TYPE AND DATES COVERED Final | |
| 4. TITLE AND SUBTITLE (Bio-Inspired theme) Bio-inspired engineering of protein-based heat sensors. | | 5. FUNDING NUMBERS F49620-01-1-0552 | |
| 6. AUTHOR(S) Todd C. Pappas | | | |
| 7. PERFORMING ORGANIZATION NAME(S) AND ADDRESS(ES) Center for Biomedical Engineering University of Texas Medical Branch 301 University Blvd Galveston TX, 77550 | | 8. PERFORMING ORGANIZATION REPORT NUMBER | |
| 9. SPONSORING / MONITORING AGENCY NAME(S) AND ADDRESS(ES) USAF/AFRL AF Office of Scientific Research 4015 Wilson Blvd Room 713 Arlington VA 22203-1954 | | 10. SPONSORING / MONITORING AGENCY REPORT NUMBER NL | |
| 11. SUPPLEMENTARY NOTES | | | |
| 12a. DISTRIBUTION / AVAILABILITY STATEMENT approve for Public Release: Distribution Unlimited | | 12b. DISTRIBUTION CODE | |
| 13. ABSTRACT (Maximum 200 Words) <p>The thermosensing organs of pit vipers are prototypical ultrasensitive biosensors for heat. Although these sensory capabilities are emergent properties of the pit organ and the CNS, the molecules responsible for thermoreception code for many of the properties of the whole receptor. Recent data suggest that thermoreceptors are heat-gated ion channel proteins. We used electrophysiology to study dissociated cultures of neurons that project to the pit organ and demonstrated <i>multiple</i> thermosensitive ion conductances in these neurons. Information on the reversal potential and rectification characteristics of these conductances verifies they are distinct. It is unclear, however, how these currents are integrated into a thermosensory response. Additionally, the kinetics of these channels could not be resolved with available temperature control systems and necessitated the design and implementation of a new rapid focal heating apparatus, now in its second phase of development. We were unable to identify homologues of the mammalian heat sensitive ion channel family (TRPV) using either low-stringency PCR or by screening a cDNA library isolated from trigeminal ganglion of the western diamondback rattlesnake. Our findings further expand the information base on thermosensation in animals and the technical tools for these studies, but we have not resolved questions of the mechanism of cellular transduction of heat in snake neurons.</p> | | | |
| 14. SUBJECT TERMS | | 15. NUMBER OF PAGES 28 | |
| | | 16. PRICE CODE | |
| 17. SECURITY CLASSIFICATION OF REPORT | 18. SECURITY CLASSIFICATION OF THIS PAGE | 19. SECURITY CLASSIFICATION OF ABSTRACT | 20. LIMITATION OF ABSTRACT |

NSN 7540-01-280-5500

Standard Form 298 (Rev. 2-89)
Prescribed by ANSI Std. Z39-18
298-102

Contents**1. Unique Thermosensitive ion conductances in pit viper trigeminal neurons. 3**

- 1.1 Introduction. 3**
- 1.2 Materials and Methods. 3**
- 1.4 Results. 5**
- 1.5 Discussion. 9**
- 1.6 References. 13**

2. Design and Testing of a Rapid Focal Hydronic Stimulator for examining electrophysiological responses of thermosensory cells. 17

- 2.1 Introduction. 17**
- 2.2 Preliminary Work. 18**
- 2.3 Design and Methods. 18**
- 2.4 Results. 19**
- 2.5 General Methods. 22**

3. Molecular Engineering of Thermosensitive Proteins. 23

- 3.1 Introduction 23**
- 3.2 Low Stringency PCR Identification of TRPV1 Homologues from Pit Viper Trigeminal Ganglion. Methods and Results. 24**
- 3.3 Directed Evolution of TRPV1 Protein. 25**
- 3.4 Methods and Results 25**
- 3.5 References 27**

1. Unique Thermosensitive ion conductances in pit viper trigeminal neurons

1.1 Introduction

Pit vipers (Viperidae: Crotalinae, rattlesnakes, copperheads) have highly evolved sensitive receptors called pit organs, which receive and relay high-resolution thermal information to the brain. This thermal information is thought to be processed and integrated at the optic tectum {Newman, 1981 110 /id} where it aids in detecting and striking prey {Noble, 1937 105 /id}. Although the pit organ has historically been studied as an infrared (IR) detector, thorough physiological {Bullock, 1956 104 /id} {de Cock, 1981 51 /id} and theoretical studies {JONES, 2001 148 /id} suggest that the organ responds to thermal rather than photonic stimuli. Our investigations of the optical sensitivity and selectivity of this organ indicate that it is responsive to a broad range of radiation from IR to ultraviolet {Moiseenkova, 2002 124 /id}. The lack of spectral selectivity strongly supports the hypothesis that the pit is a highly sensitive thermoreceptor rather than photonic IR detector.

The pit organ shows structural specializations indicative of a high-resolution thermal detector. The temperature sensing terminal nerve endings innervate an ultra-thin (<25 μm) pit membrane {Noble, 1937 105 /id} that acts as the heat-sensing surface. This thin membrane and the associated terminal nerve mass are suspended in a facial cavity in front of an inner air space, giving the pit organ an extremely low thermal mass. The pit organ also has a rich capillary network that is thought to act as a rapid heat sink {Goris, 2000 12 /id}. This combination of low thermal mass and rapid heat dissipation contributes to the precise temporal and spatial resolution of thermal stimuli. Multiple and single-unit neuronal activity recorded from pit organ afferents demonstrate that these receptors are sensitive to very small temperature changes (about 0.003°C){Bullock, 1956 104 /id}, and can transmit this thermal information over a broad range of temperatures (15°-37°C). This suggests that the pit organ must have highly-sensitive neurons and ion channel mechanisms capable of receiving and transmitting thermal information and that these complement the anatomical specializations of the pit organ for heat reception. However, the cellular and molecular machinery responsible for converting temperature information into neuronal signals in the pit organ is completely unknown.

A generator potential for thermal stimuli at the pit organ has been identified using extracellular recordings {Terashima, 1968 59 /id}, and this supports the hypothesis that the terminal nerve mass may express temperature-sensitive integral membrane proteins. This is also consistent with reports on mammalian thermoreceptors, especially thermal nociceptors, where the activation-temperature threshold, ion conductance, and even behavioral features {Caterina, 1997 9 /id} {Caterina, 2000 139 /id} have been correlated to the presence of a temperature-gated cation channel TRPV1. Thermal nociceptive neurons are fairly plentiful, and thus benefited studies linking TRPV1 to thermal responses. The snake pit organ is a unique system for the study of these lower temperature- threshold thermoreceptors because it has the highest known density of warm receptors {Bullock, 1957 125 /id} and there are far fewer “warm” receptors in mammals {Lynn, 1982 140 /id} {Hellon, 1982 141 /id} {Bullock, 1956 104 /id}. By analogy to TRPV1, ion conductances corresponding to warm receptors may be abundant in neurons that project to the pit organ.

Here we demonstrate for the first time that dissociated neurons from the pit viper TG, which supplies the pit organ {Bullock, 1957 125 /id}, shows a heat-sensitive current with a temperature threshold and biophysical properties unlike those identified in mammalian neurons. Voltage clamp recordings revealed an inward monovalent cation current, I_{AT} , which increased with heating and tracked temperature change. I_{AT} was found in a large proportion of TG neurons that were isolated and had a threshold of about 18°C.

1.2 Materials and Methods

Animals. Copperheads (*Agkistrodon contortrix*), Western Diamondback rattlesnakes (*Crotalus atrox*), and common garter snakes (*Thamnophis sirtalis*) were caught wild and obtained from a commercial dealer (Glades Herp, Myers FL). *A. contortrix* weight ranged from 100-500 gm, *C. atrox*

DISTRIBUTION STATEMENT A

Approved for Public Release
Distribution Unlimited

20050519 105

from 400-800 gm, and *T. sirtalis* was less than 100 gm. Snakes were individually housed in either glass aquariums or transparent plastic containers. All containers were supplied with a water bowl, hiding box, and a rock and were placed on a thermal strip to allow for behavioral thermoregulation. The housing room was maintained at an ambient temperature of 24-28°C and a 12/12 light/dark cycle. Animals were fed freshly euthanized baby mice once monthly. All procedures involving the use of animals were conducted in accordance with the "Guide for the Care and Use of Laboratory Animals" published by the National Institutes of Health (NIH publication 85-23, revised 1985).

Culture of Trigeminal Ganglion. Cell bodies that have sensory terminal nerve specializations in the infrared/heat-sensitive pit organ are found in the ganglia of ophthalmic, maxillary, and mandibular branches of the trigeminal nerve {Bullock, 1957 125 /id}. Snakes were anesthetized with Isofluorane USP (Abbott Laboratories, North Chicago IL) then decapitated and the head was placed on ice to minimize cell death after decapitation. The TG was located visually, removed, and placed in ice-cold F12:DMEM (Gibco BRL). Cells were dissociated from the ganglia by treatment with collagenase (1 mg/mL, 45 min, 28°C) and trypsin (2.5 mg/mL, 5 min, 22°C) followed by mechanical dissociation with plastic pipettes. The dissociated cell mixture was layered onto 25 % percoll (Sigma Chemical Co, St Louis MO) and centrifuged for 10 min at 500 xg to remove large cell bodies and debris {Goldenberg, 1983 90 /id}. Cells were cultured in F12:DMEM supplemented with 10% fetal bovine serum, 10 U/mL penicillin, 10 µg/mL streptomycin (Gibco BRL) and 2 mM glutamine (Gibco BRL) on poly-D-lysine coated coverslips or in treated 12-well tissue culture plates (BD Falcon). Cells were maintained at 28°C in 7% CO₂/93% air for 16-96 hrs.

Electrophysiology. Recordings from neurons were made in HEPES-buffered saline (HBS, in mM: NaCl 130, KCl 3.0, CaCl₂ 2.0, MgCl₂ 1.2, HEPES [pH 7.3] 10, glucose 10). Neurons were voltage clamped using single patch electrodes in the whole-cell mode {Hamill, 1981 123 /id} and held at -65 mV using an Axon Instruments model 200A amplifier. Patch pipettes were made from 1.65 mm OD 7052 glass (Garner Glass) and pulled to a resistance of 2-5 MΩ using a Sutter Instruments P 87 puller. Patch electrode solutions contained 140 mM K-gluconate, 2 mM MgCl₂, 2 mM 1,2-bis (2-aminophenoxy) ethane- N,N,N',N'-tetraacetic acid (BAPTA), 0.2 mM CaCl₂, and 1 mM HEPES with a pH 7.4. K-gluconate was substituted with CsCl for reversal potential experiments. Ion permeability ratios were calculated using modifications of the Goldman-Hodgkin-Katz equation {Lewis, 1979 151 /id}. Voltage clamp protocols were controlled using the pCLAMP (v. 6.2, Axon Instruments) suite of programs, and current traces were filtered using algorithms supplied in the software. Statistical analyses were preformed using StatView (ver. 5.0.1, SAS Institute Inc., Cary NC).

Calcium Imaging. Simultaneous voltage clamp and intracellular Ca²⁺ level determinations were made using the perforated patch technique on fura-2-loaded neurons {Zhou, 1993 127 /id}. Neurons were loaded with 5 µM fura-2 AM (Molecular Probes) in HEPES buffered saline at room temperature for 1 hour. Patch pipettes were loaded with an electrode solution consisting of (in mM): KCl 30, K₂SO₄ 65, HEPES 10, pH 7.4, and EGTA 1. Amphotericin B (Sigma) at a final concentration of 0.5 µg/ml was used in the internal solution to provide access to the cell. Gigaohm seals were placed on neurons and cells were voltage clamped at -65 mV. Cell access was monitored by observing the change in cell capacitance and membrane currents during a -15 mV voltage step. The preparation was illuminated with a 75W xenon light source attached to a beam splitter (Oriel, Stratford CT) that directed light through a 340 nm or a 380 nm filter. A dichroic filter (510 nm) directed the illumination to the neurons through a 100X oil immersion lens (n.a. 1.3) and a photomultiplier tube (Oriel) quantified fluorescence emission above 510 nm. Fluorescence emission data from excitation at 340 nm and 380 nm were collected every 1.55 s.

1.4 Results

We performed whole-cell voltage clamp recordings on neurons cultured from the TG. Our primary culture technique yielded neurons and other cells that were < 60 µm in diameter, the size of neurons we recorded from was 30 ± 9 µm (SD, n=157). Neurons were identified morphologically as

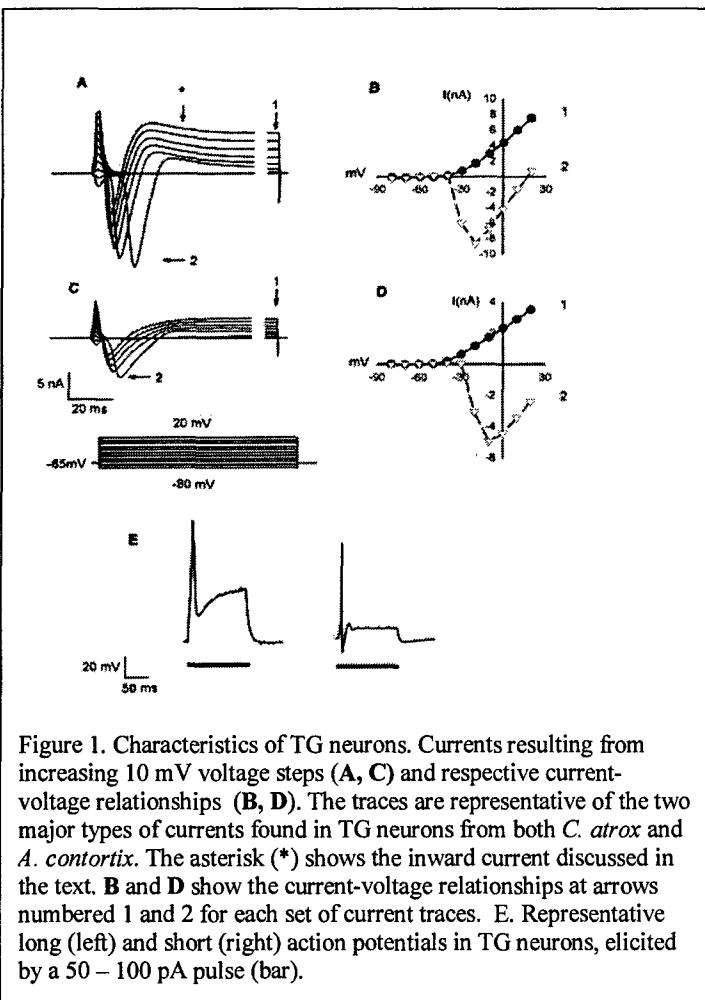


Figure 1. Characteristics of TG neurons. Currents resulting from increasing 10 mV voltage steps (A, C) and respective current-voltage relationships (B, D). The traces are representative of the two major types of currents found in TG neurons from both *C. atrox* and *A. contortrix*. The asterisk (*) shows the inward current discussed in the text. B and D show the current-voltage relationships at arrows numbered 1 and 2 for each set of current traces. E. Representative long (left) and short (right) action potentials in TG neurons, elicited by a 50–100 pA pulse (bar).

showing spontaneous action potentials (APs) under current clamp. However, in 14 of 19 neurons (74%) from *A. contortrix*, we were able to elicit action potentials (APs) under current clamp with a 50–100 pA, 100 ms anodic current injection (Figure 1E). We recorded two types of APs, which could be distinguished by having a short (mean = 5.4 ± 1.2 ms, SD, n=9) or long (mean = 17.1 ± 1.7 ms, SD, n= 5) spike duration. Due to the low number of temperature-unresponsive neurons in this sample, we were unable to determine if the distribution of AP type was nonrandom with respect to the temperature response characteristics of the neuron.

Temperature responses were elicited by applying heated or chilled HBS as close as possible to the voltage clamped neuron using a polypropylene Pasteur pipette. A thermocouple with rapid temperature response (Physitemp, Clifton NJ) placed within 500 μ m of the cell was used to estimate the thermal stimulus delivered to the cell. We determined heating and cooling parameters from 30 representative temperature records in which we sought to determine the current response of neurons to a temperature step. Representative temperature traces are presented in the top panels of Figure 2A-C. The cells were heated from a resting room temperature of $20.4 \pm 1.4^\circ\text{C}$ (SD) to a final temperature of $34.5 \pm 4.8^\circ\text{C}$ (range 27–49°C) at a mean rate of $3.3 \pm 1.8^\circ\text{C}/\text{s}$. The duration of the elevated temperature step was variable but always greater than 10s, during which there was ambient cooling at a rate of $0.17 \pm 0.05^\circ\text{C}/\text{s}$. The cells were then cooled with chilled HBS at a rate of $2.0 \pm 1.0^\circ\text{C}/\text{s}$ back to baseline temperature to show reversal of the response.

Temperature-responsive neurons were defined as having consistent, temporally correlated responses to stimulation and having an inward current of at least $2.0 \text{ pA}^\circ\text{C}$ when heated to a minimum of 10°C from room temperature ($\sim 20^\circ\text{C}$). These currents also needed to reverse upon cooling. Using these criteria, we identified 75% (18 of 24) of the TG neurons in *C. atrox* and 74% (90 of 122) in *A. contortrix* as temperature-responsive (Table 1, Figure 2A,B). Figure 2A-C shows

phase-bright cells that showed voltage-dependent conductances when 10 mV voltage steps from -90 to +20 mV (100 or 300 ms) were applied (Figure 1). Under our culture conditions, neurons did not typically express neurites. Table 1 presents general characteristics recorded from these cells. Figure 1A and C show the two general current responses we recorded from these neurons, with the current voltage relationships shown in Figure 1B and D, respectively. These currents differed only in having a rapid inward component following voltage-dependent outward currents (Figure 1A, asterisk). The input resistance (R) of neurons of the three species tested was determined from the slope of current voltage relationships from -90 to -60 mV and is presented in Table 1. A two-way analysis of variance shows no significant difference in input R among species tested ($F_{2,46} = 0.69$, $p > 0.05$) or between temperature-unresponsive and temperature-responsive neurons (see below for criteria, $F_{1,46} = 0.51$, $p > 0.05$).

We did not observe cells

representative inward current responses to application of warmed HBS to TG neurons from all species tested. We called this current I_{AT} . The current responses were rapid, temperature-dependent, and followed temperature changes closely. Figure 2D shows a representative response from a temperature unresponsive cell, showing no significant current change due to the application of heated HBS. In temperature-responsive cells, inward current in response to heat was accompanied by a decrease in membrane potential when recorded under current clamp conditions (Figure 2E). Heating and cooling of TG neurons did not result in the generation of action potentials.

I_{AT} recorded in *C. atrox* and *A. contortrix* were very similar (Table 1). The magnitude of I_{AT} was $15.6 \pm 11.7 \text{ pA}^\circ\text{C}$ (SD, n=13) in TG neurons from *C. atrox* and $11.2 \pm 14.2 \text{ pA}^\circ\text{C}$ (n=36) in TG neurons from *A. contortrix*. The range was 3.9 to 45.4 pA°C for *C. atrox* and 2.15 to 63.7 pA°C for *A. contortrix*. We calculated current density of I_{AT} based on the assumption that TG neurons were spherical, with a surface area determined by the formula

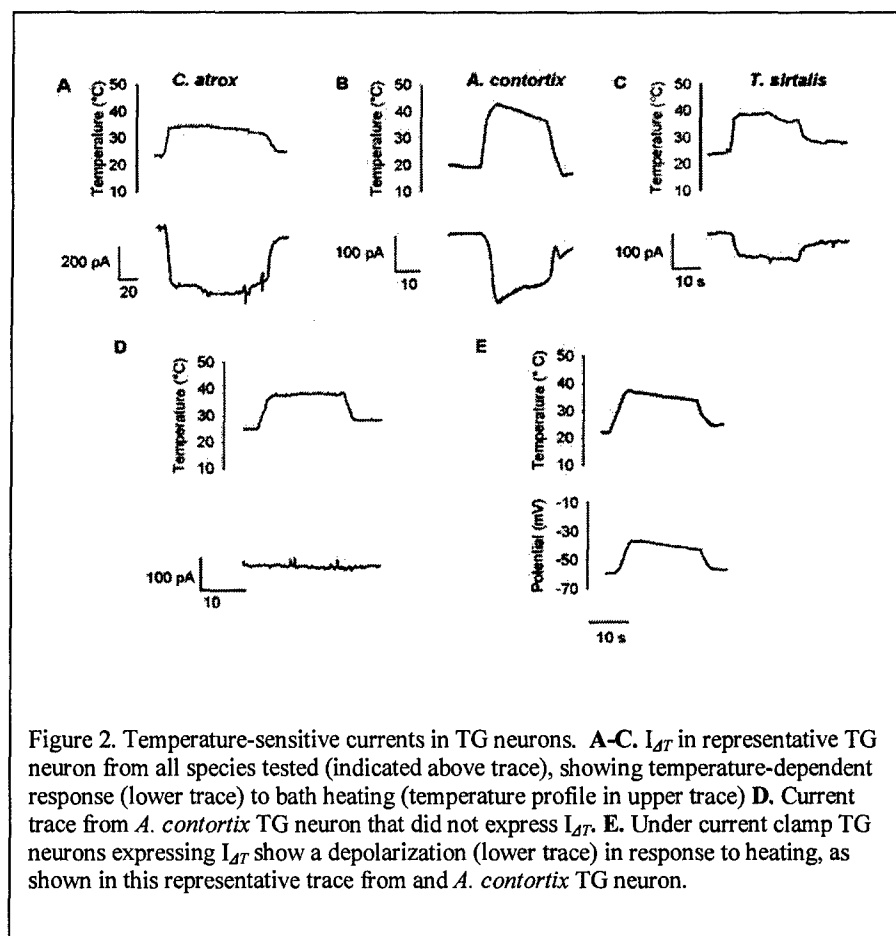


Figure 2. Temperature-sensitive currents in TG neurons. A-C. I_{AT} in representative TG neuron from all species tested (indicated above trace), showing temperature-dependent response (lower trace) to bath heating (temperature profile in upper trace). D. Current trace from *A. contortrix* TG neuron that did not express I_{AT} . E. Under current clamp TG neurons expressing I_{AT} show a depolarization (lower trace) in response to heating, as shown in this representative trace from an *A. contortrix* TG neuron.

Table 1. Characteristics of TG neurons

| Species | <i>C. atrox</i> | <i>A. contortrix</i> | <i>T. sirtalis</i> |
|--|------------------------|------------------------|---------------------------------|
| Total neurons | 30 | 165 | 20 |
| Temperature Responsive (%) | 18 (75%) | 90 (74%) | 3 (15%) |
| Temperature Unresponsive | 6 | 32 | 17 |
| Diameter [μm , mean \pm SD, (n)] | | | |
| Responders | 32 ± 12 (16) | 30 ± 8 (76) | 47 ± 6 (3) |
| Non responders | 33 ± 12 (6) | 30 ± 8 (25) | 35 ± 10 (16) |
| Input Resistance [$M\Omega$, mean \pm SD (n)]* | | | |
| Responders | 354 ± 246 (11) | 540 ± 259 (19) | 371 ± 272 (3) |
| Non responders | 392 ± 131 (2) | 681 ± 160 (4) | 468 ± 266 (13) |
| I_{AT} current magnitude [pA°C , (n)] | 15.6 ± 11.7 (13) | 11.2 ± 14.1 (36) | 3.5 ± 2.5 (3) |
| I_{AT} current density [$\text{nA}^\circ\text{C}/\text{cm}^2$, mean \pm SD (n)] | 514.4 ± 639.3 (11) | 611.6 ± 649.3 (20) | 46.9 ± 3.0 (3) [†] |

* Two-way ANOVA showed no significant effects of species ($F_{2,46} = 0.69$ p>0.05) or responsiveness ($F_{1,46} = 0.51$, p>0.05) nor an interaction effect ($F_{2,46} = 0.24$ p > 0.05).

[†] ANOVA showed significant effect of species on I_{AT} current density ($F_{2,31} = 6.65$, p < 0.01). Scheffe's multiple contrast showed that current density was significantly different in neurons from *T. sirtalis* when compared either to those of *C. atrox* (p< 0.01) or *A. contortrix* (p< 0.01)

$4\pi r^2$. The values for surface density are expressed as nA/ $^{\circ}\text{C}/\text{cm}^2$ and are presented in Table 1 for the species tested. Current densities showed high variability and were \log_{10} transformed for statistical comparisons {Zar, 1984 116 /id}. There was no statistical difference in I_{AT} current density in TG neurons of *C. atrox* vs. *A. contortrix*. We pooled data from both snakes to examine the effect of cell size on

current density. There was a weak but statistically significant negative correlation {Zar, 1984 116 /id} between neuron surface area and the \log_{10} transformed current density value ($r = 0.49$, $s_r = 0.16$, $n = 31$, $t = 3.03$, p<0.05), indicating that smaller cells tend to express more I_{AT} .

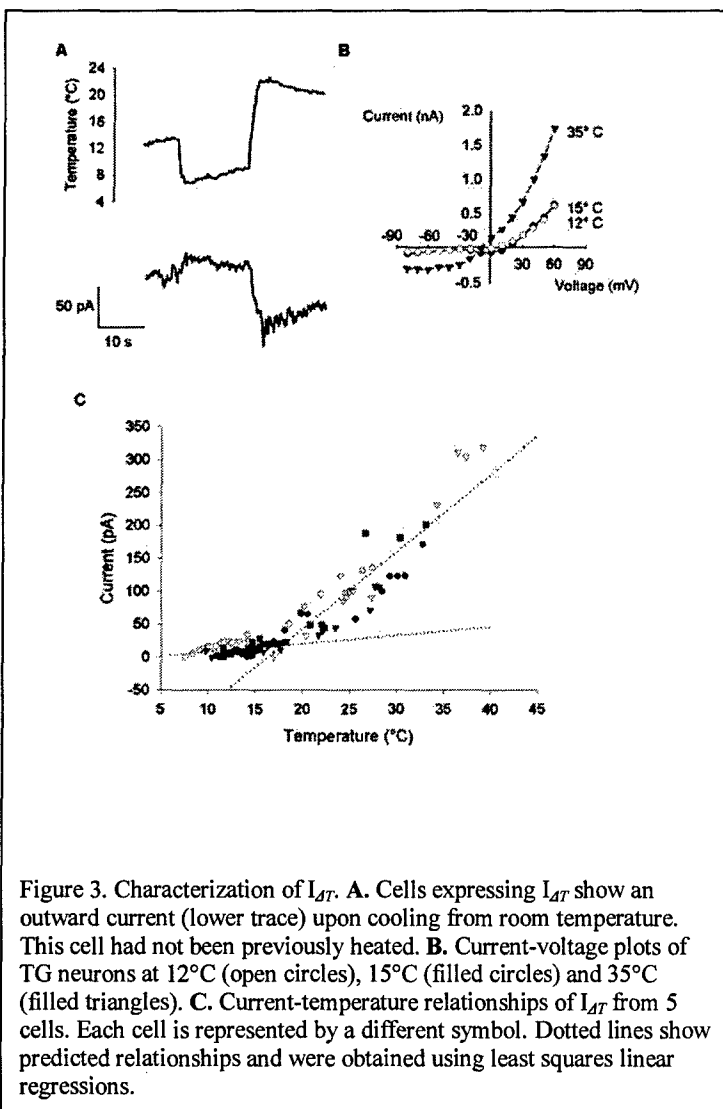
We also examined heat-responsive currents in TG neurons from the common garter snake (*T. sirtalis*, Figure 2C, Table 1), a snake that does not have specialized heat sensing organs, but is in the same superfamily (Xenophidia) as the crotaline snakes. TG neurons were isolated and recorded from 3 different snakes. Temperature-activated currents resembling I_{AT} were seen in 3 of 20 TG neurons (15%) from *T. sirtalis*. It was possible to make a statistical comparison between the proportions of I_{AT} -expressing neurons in the pooled population of *C. atrox* and *A. contortrix* TG neurons vs. those of *T. sirtalis* because the sample sizes were within conservative estimates necessary to maintain statistical power for comparisons of unequal samples {Zar, 1984 116 /id}. The crotalines had a significantly greater proportion of I_{AT} containing neurons in their TG than *T. sirtalis* (one-tailed test for significant of proportions, $Z = 6.87$, p<0.01).

Additionally, TG neurons from *C. atrox* or *A. contortrix* had a significantly higher I_{AT} current density than TG neurons from *T. sirtalis* (see Table 1 for statistical information).

Cooling cells from RT revealed that I_{AT} is activated within the range of temperatures that a pit

Figure 3. Characterization of I_{AT} . A. Cells expressing I_{AT} show an outward current (lower trace) upon cooling from room temperature. This cell had not been previously heated. B. Current-voltage plots of TG neurons at 12°C (open circles), 15°C (filled circles) and 35°C (filled triangles). C. Current-temperature relationships of I_{AT} from 5 cells. Each cell is represented by a different symbol. Dotted lines show predicted relationships and were obtained using least squares linear regressions.

viper would encounter in the wild {Wills, 2000 126 /id} (Figure 3A). We examined current voltage relationships of cells that were first cooled to 12-15°C before heating to determine the temperature at which I_{AT} was inactive. Cells cooled to 12-15°C showed no further temperature-dependent changes in current, suggesting I_{AT} was inactive in this range (Figure 3B). The current temperature relationship



of I_{AT} from *A. contortrix* is shown for 5 cells presented in Figure 3C. These cells were chosen because they had stable I_{AT} data over a large range of temperatures and current values were subtracted from the baseline that represented the lowest value over the record. The I_{AT} vs. T relation showed a nonlinear response, with little current increase at lower temperatures (10-15°C) transitioning to a more rapid rate of increase at just below 18°C. Regression lines for the two components were predicted by least squares method minimizing the trend in residuals {Zar, 1984 116 /id} and the threshold was determined to be 17.8°C for the steeper current gain per unit temperature.

The reversal potential (RP) of I_{AT} was determined for TG neurons from *A. contortrix* by subtracting currents generated from increasing voltage steps at 15°C from those resulting from heating neurons to 26-35°C (Figure 4A). We use CsCl electrodes to reduce the contribution of voltage activated K⁺ channels, which may influence the value

of the RP {Adams, 1980 128 /id}. The RP of I_{AT} was -12.7 ± 9.6 mV (SD, n=9). Similarly, cells held at and above 0 mV showed a reversal of the heat-induced current (Figure 4B). Consistent with the RP, ion substitution experiments indicated that heat may activate a monovalent cation channel with K⁺ permeability. Substitution of NaCl with equimolar N-methyl D-glucamine resulted in a 49% ($\pm 26\%$ SD, n=4) decrease in the magnitude of the integrated I_{AT} current per °C (Figure 5A). More detailed ion substitution experiments are summarized in Table 2. Voltage ramps were used to examine RP of neurons in varying ionic conditions. The RP of I_{AT} in 10 mM NaCl shifted to -27.9 ± 4.0 mV (Table 1) from -12.7 mV. Interestingly, increasing CaCl₂ from 2 mM to 10 mM had no effect on the RP of I_{AT} (-24.8 ± 3.2 mV, SD, n=3) from cells in 10 mM NaCl. Similarly, a ten-fold reduction in Ca²⁺ did not affect the RP in 120 mM NaCl. From these data, and estimated intracellular concentrations of Na⁺ and K⁺ of 4 and 140 mM, respectively, we determined that for I_{AT} the relative permeability P_K/P_{Na} ≈ 1.16 from the Goldman, Hodgkin and Katz voltage equation {Hille, 2001 154 /id}.

In order to verify the lack of Ca²⁺ permeability in I_{AT} suggested by ion substitution experiments, we measured intracellular Ca²⁺ using fura-2 in 43 voltage clamped TG neurons from *A. contortrix*. I_{AT} -expressing TG neurons did not show an increase in intracellular Ca²⁺ (Figure 5B),

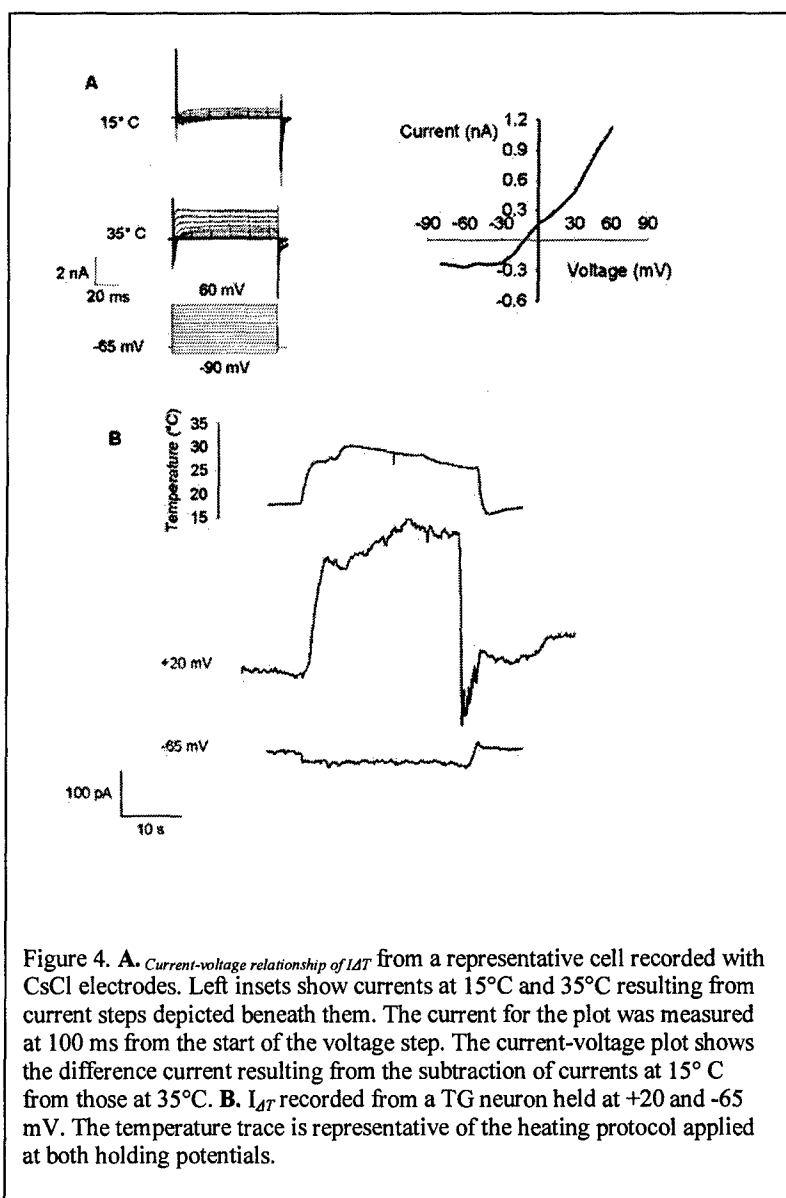


Figure 4. A. Current-voltage relationship of I_{AT} from a representative cell recorded with CsCl electrodes. Left insets show currents at 15°C and 35°C resulting from current steps depicted beneath them. The current for the plot was measured at 100 ms from the start of the voltage step. The current-voltage plot shows the difference current resulting from the subtraction of currents at 15°C from those at 35°C. B. I_{AT} recorded from a TG neuron held at +20 and -65 mV. The temperature trace is representative of the heating protocol applied at both holding potentials.

further indicating that these heat-activated channels are impermeable to Ca^{2+} . From these data it can be assumed that I_{AT} is primarily a monovalent cation conductance.

Previous research has established the pharmacological identity of several temperature-sensitive ion channels {Caterina, 1997 9 /id; Jung, 1999 7 /id; Liu, 2000 10 /id; McKemy, 2002 122 /id}. We exposed I_{AT} -expressing TG neurons from *A. contortrix* to 10 μM capsaicin (in 0.001% [vol/vol] ethanol) to examine if a pharmacologically active TRPV1 homologue is present in these cells {Caterina, 1997 9 /id}. Cells did not respond to capsaicin, nor was the magnitude of response to

heat stimulus changed ($n=4$). Similarly, amiloride, which blocks temperature sensitive ENaC channels {Askwith, 2001 146 /id} had no effect on the magnitude of I_{AT} in TG neurons ($n=5$).

The TG also had cooling sensors. We identified 7 neurons that responded to cooling with a rapid and transient inward current, I_{CoolA} (Figure 5). I_{CoolA} was recorded independently on 6 cells and on one cell that also showed I_{AT} . I_{CoolA} was activated when cells were cooled either from RT or after having been heated (Figure 5a), suggesting a response to cooling regardless of starting temperature. The threshold for activation of I_{CoolA} was highly variable, having a mean of 26.0 °C (± 3.5 SD $n=16$ responses) and a range of from 19.3

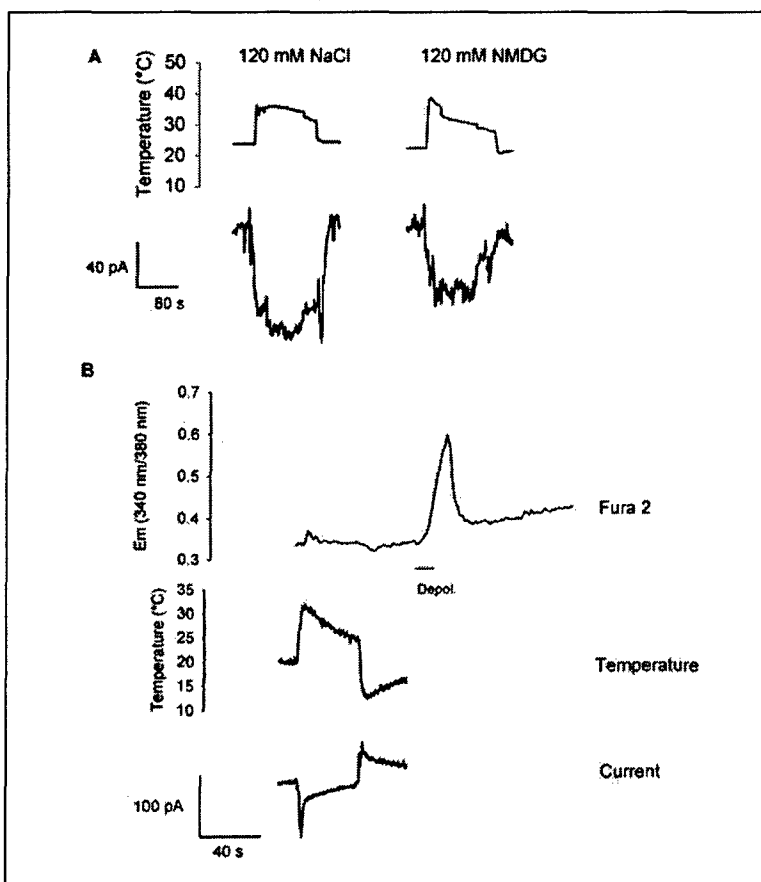


Figure 5. A. Sodium dependence of I_{AT} . TG neurons were voltage clamped at -65 mV in HBS and I_{AT} was recorded in response to application of warmed HBS. The recording media was changed to one in which 120 NMDG was substituted for NaCl, and the cell was heated by application of the substituted media. B. Calcium permeability of the heat-activated current was monitored using fura-2 spectrophotometry and whole-cell voltage clamping simultaneously. This panel shows simultaneous fura-2, temperature and current data for a representative heat responsive TG neuron. TG neurons loaded with fura-2 show no heat induced change in the ratio (stimulation at 340nm/380 nm) of fluorescence emission at 510 nm. The neuron was depolarized (bar) by turning off the holding potential, and this resulted in a strong signal, indicating that cells were loaded and responsive to intracellular Ca^{2+} level changes. Temperature and current data were not taken just prior to and after the positive control depolarization, but off-line monitoring of temperature show there was no deviation from baseline (20°C).

to 31.0 °C among the cells and up to 6.2 °C within a cell. I_{CoolA} reversed at positive holding potentials (Figure 5b), suggesting unique ion dependencies from those of I_{AT} .

1.5 Discussion

We have recorded a novel temperature activated current in neurons that supply the pit organ of *A. contortrix* and *C. atrox*. The current was novel in that it had the lowest threshold of activity of any

known heat-activated conductance, and had ion permeability unlike that of any characterized temperature sensitive channel. I_{AT} was a monovalent cation conductance that was active at ambient temperatures and increased in response to heating. The effective temperature range of I_{AT} was consistent with having a role in sensitive thermal detection of prey and other environmental stimuli. I_{AT} was found in a large proportion of the neurons in the TG of *C. atrox* and *A. contortrix*. Temperature activated neurons were also found in the TG of snakes lacking the pit organ (*T. sirtalis*), but at a much lower frequency and with lower current density. This suggests that crotaline snakes may have adapted a general warm thermosensor to a specialized function as neuronal signal transducers in a highly sensitive thermoreceptive organ. The ion dependence of I_{AT} was found to be different from other known temperature-sensitive channels {Caterina, 1997 9 /id} {McKemy, 2002 122 /id} {Xu, 2002 121 /id} {Guler, 2002 119 /id}, further illustrating the unique nature of these temperature gated conductances.

The presence of a large number of neurons expressing

Table 2. Ion substitution and reversal potentials of I_{AT}

| (mV) Na ⁺ | External Cations (mM) | | Reversal Potential (mV) |
|-------------------------|-----------------------|------------------|------------------------------|
| | NMDG | Ca ²⁺ | |
| 120 | 0 | 2 | -12.7 |
| ± 9.6 | | | |
| 120 | 0 | 0.2 | -11.7 |
| ± 5.9 | | | |
| 10 | 110 | 2 | -27.9 |
| ± 4.0 | | | |
| 10 | 110 | 10 | -24.8 |
| ± 3.2 | | | |

temperature-gated currents in these cells further strengthens the hypothesis that heat detection in the pit organ is not due to photonic IR detection but is a result of highly-sensitive heat detection {Bullock, 1956 104 /id} {de Cock, 1981 51 /id} {Moiseenkova, 2002 124 /id}.

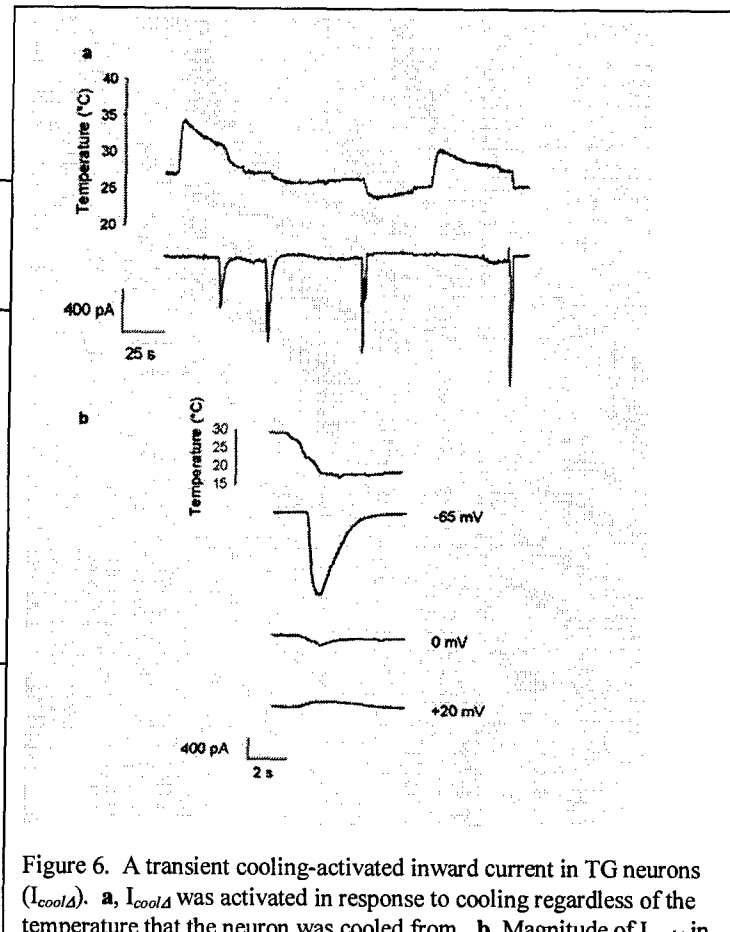


Figure 6. A transient cooling-activated inward current in TG neurons (I_{coolA}). a, I_{coolA} was activated in response to cooling regardless of the temperature that the neuron was cooled from. b, Magnitude of I_{coolA} in a TG neuron at different holding potentials. The temperature trace is representative of the heating protocol applied at all holding potentials.

The use of *in vitro* preparations to study thermoreceptors

A generator potential for pit thermoreceptors has been recorded from crotaline snakes including *Agkistrodon* {Terashima, 1968 59 /id}. Terashima and colleagues {Terashima, 1968 59 /id} recorded both voltage spikes and slow potentials using extracellular electrodes inserted just below the pit membrane into the terminal nerve mass. These potentials were proportional to stimulus intensity and duration, but drifted in direction due to the instability of the preparation. We chose to use a voltage clamp to obtain more detailed biophysical information on temperature-activated currents, but we were unable to clamp the terminal nerve mass, which probably contains the highest density of cellular structures that cause temperature dependent currents (i.e., heat-sensitive ion

channels). Recordings were taken from cell bodies because of their ease of preparation and because temperature responses of neurons have been shown to be accurately replicated in cultured trigeminal and dorsal root ganglion neuron cell bodies {Liu, 2000 10 /id} {Cesare, 1996 130 /id} {Reichling, 1997 129 /id} {Nagy, 1999 89 /id}. This is because heat sensitive ion channels are expressed and active at the cell body in cultured neurons.

Neurons were subjected to a wide range of temperatures during these recording procedures, and some of these neurons showed no response to temperature change. This is consistent with findings in ganglion cultures from mammalian sensory neurons where there was a clear distinction between temperature-sensitive and insensitive cells, and suggests that there was not artifactual temperature induced activation of resting leak or voltage activated currents with thermal stimulus. Cells expressing I_{AT} showed characteristic nonlinear relationship between temperature and currents that indicated a threshold just below 18°C. This type of current-temperature relationship has been seen for temperature-activated currents {Vyklicky, 1999 131 /id} and for isolated temperature-gated ion channels from mammals {Caterina, 1997 9 /id} {McKemy, 2002 122 /id} {Xu, 2002 121 /id}. The transition from slow to rapid current change as a function of temperature is thought to happen at the temperature in which there is a rapid and reversible change in the ion channel, possibly associated with temperature-dependent gating of the channel {Vyklicky, 1999 131 /id}.

We could not record APs in response to heating of TG neurons, although it is clear from studies on intact preparations that heat sensation in the pit organ is transmitted via APs. It is possible that the rate of heat stimulus we presented to these cells was too slow to generate APs. Temperature changes in the low thermal mass pit organ should be nearly instantaneous, even if they are small. With slow changes, however, ion channels responsible for stimulating regenerative changes in membrane potential might be inactivated before the AP could take place, or voltage-activated channels responsible for terminating APs might be activated before the I_{AT} could significantly change the membrane potential. Two previous studies {Bullock, 1956 104 /id} {de Cock, 1981 51 /id} suggest that pit afferents respond to the rate of temperature change as well as the stimulus intensity. However, changes in AP frequency could be distinguished even with very long temperature rise times {Bullock, 1956 104 /id}. It is also possible that the density of I_{AT} in dissociated TG neurons was not sufficient to give rise AP-producing depolarization of membrane potential, or that accessory channels involved in AP production in these cells were not adequately expressed. This could be the result of low or altered expression of putative ion channel(s) responsible for I_{AT} lowered or altered AP-associated ion channels in dissociated cell culture. Finally, it is possible that the role of I_{AT} is not to produce fast enough or robust enough depolarization for AP activation, but instead modulate ongoing changes in membrane potential. This is supported by studies from pit viper trigeminal nerve {Bullock, 1956 104 /id} {de Cock, 1981 51 /id} and trigeminal ganglion neurons {Terashima, 1991 149 /id} showing that these elements are spontaneously active and that temperature change is signaled by alterations in ongoing spike activity. We did not see spontaneous APs in our cells, possibly as a result of dissociated culture, but we speculate that one mechanism by which I_{AT} might signal heat is to produce a slow depolarization that increases spike frequency, as has been described for other sensory systems {Burgoon, 2001 153 /id; Doiron, 2003 152 /id}.

Neurons expressing a temperature-sensitive current similar to I_{AT} were also found in the TG from the common *T. sirtalis*, a snake that does not have a specialized organ for sensitive heat detection, but at a significantly lower frequency and with lower current density. It is not surprising that we found thermosensitive cells in the TG from this snake, as this ganglion supplies more general temperature sensors to the face {Bullock, 1957 125 /id}. It is also possible that some of the temperature-responsive neurons we recorded from the *C. atrox* and *A. contortrix* TG are actually cutaneous warm receptors that did not send projections to the pit organ, but to other parts of the face. If this is the case then the frequency of cells expressing I_{AT} we observed in the TG is not an accurate estimate of the frequency of warm-receptive neurons sending projections to the pit organ but instead to the entire facial region innervated by the trigeminal nerve. The frequency of TG cells showing various temperature-activated currents that actually send afferents to the pit organ will have to be determined using retrograde labeling from the pit organ in conjunction with physiological recordings

in the TG. However, a comparison can be made with the frequency of warm-receptive neurons found in the TG of the *T. sirtalis*, as both estimates were made using the same sampling procedure. The fact that I_{AT} in *T. sirtalis* was qualitatively similar to that of pit vipers has interesting implications in the evolution of the pit organ and its thermosensitivity. The pit afferents of crotaline snakes have been shown to have a higher number of warm-sensitive fibers than any known animal {Bullock, 1956 104 /id}. Our data on proportion of heat sensitive neurons in pit vipers vs. *T. sirtalis*, are consistent with these findings. Additionally, our data also showed that the current density of I_{AT} is much higher in pit vipers than in *T. sirtalis*. It is possible that pit viper thermosensors evolved as specializations of general cutaneous warm receptors like those that would be found in all snakes. The evolution of a specialized pit organ was accompanied by an expansion of numbers of warm-sensitive neurons supplying the area, resulting in very high thermal sensitivity of the pit organ. Additionally, individual neurons may be more sensitive to temperature, and this would result in these neurons having greater electrophysiological responses to temperature change further enhancing sensitivity of an integrated thermoreceptor like the pit.

I_{AT} correlates with behavioral data on snake thermosensing

The concordance in temperature response characteristics between behavioral or nerve recordings and cultured neuronal preparations has often been used to establish a causal link between temperature sensation and temperature-activated currents {Cesare, 1996 130 /id}. Our data from snake TG neurons correlated to features discovered from behavioral, whole nerve, or single fiber recordings from pit vipers. Most notably the temperature threshold for I_{AT} in pit viper TG was in good agreement with recordings from the pit afferent nerves that showed loss of spontaneous spiking activity at 10-15°C {de Cock, 1981 51 /id}. Above this threshold there was a constitutive inward current, which may be related to "background" activity of nerves seen above 18°C. The temperature tracking characteristics of I_{AT} may also be related to the non-adapting spike discharge seen in pit afferents when the pit is heated. The detailed investigations of de Cock Buning *et al.* (1981) demonstrate that rapid adaptation of spiking frequency is a property of rapid cooling in the low thermal mass pit organ and not an adaptation at the nerve itself. Adding water to the pit increased its thermal mass and resulted in a non-adapting discharge of pit afferents. This suggests that the neural response is constant throughout the thermal stimulus and is in agreement with the behavior of I_{AT} . The temperature tracking characteristics of I_{AT} were also consistent with the slow, continuous temperature dependent changes seen in the extracellular generator potentials recorded at the pit membrane {Terashima, 1968 59 /id}.

Behavioral data also shows that pit afferents stop firing above 37°C {de Cock, 1981 51 /id} and this does not correlate well with the behavior of I_{AT} , which showed responses even at and above 40°C. This raises the possibility that there may be other temperature-sensitive currents that mediate thermosensitivity at the pit organ. It is possible that there may be a high-threshold temperature-sensitive current that responds at temperatures above 37°C and may be involved with the cessation of the pit response at these temperatures. We already have preliminary data that suggest that the TG may contain neurons that have a transiently-activated cooling-sensitive current that may contribute to the sensitivity described in snake thermosensing {Pappas, 2002 145 /id}.

Similarities and differences between I_{AT} and currents from temperature-sensitive ion channels

The hypothesis that a heat-sensitive ion conductance, similar to the one found here for the snake, is a transducer of thermal information has also been proposed and investigated for mammalian primary thermosensory neurons *in vitro* {Reichling, 1997 129 /id} {Nagy, 1999 89 /id} {Liu, 2000 10 /id}. In some neurons, currents evoked at the level of thermal nociception ($\cong 42^\circ\text{C}$) can also be mimicked by capsaicin {Caterina, 1997 9 /id} {Liu, 2000 10 /id} {Nagy, 1999 89 /id}, the noxious ingredient of hot peppers that can elicit a similar thermal sensation, and can be partially blocked by antagonists for capsaicin binding {Savidge, 2001 142 /id}. This feature has allowed investigators to isolate a temperature-responsive ion channel, TRPV1, by expression cloning {Caterina, 1997 9 /id}, and identify a cold sensitive channel by similar methods {McKemy, 2002 122 /id}. Homology

screening has revealed a number of temperature-sensitive channels in the transient receptor potential (TRP) family of integral membrane proteins that respond over a broad range of temperatures {Caterina, 1997 9 /id} {McKemy, 2002 122 /id} {Xu, 2002 121 /id} {Guler, 2002 119 /id}. Although neither the pit organ {Moiseenkova, 2002 124 /id} nor our I_{AT} -expressing TG neurons show capsaicin sensitivity, this does not preclude that I_{AT} could arise from a TRPV1 homolog or ortholog, as shown within chicken {Jordt, 2002 143 /id} and bullfrog {Kuffler, 2002 150 /id} DRG neurons, respectively. The similarity of some temperature response characteristics of I_{AT} to those of members of the TRP family suggests that I_{AT} may arise from a single, temperature-gated ion channel homologous to one of the TRP proteins. I_{AT} shows similar current-voltage relationship both in terms of its reversal potential and its rectification {Caterina, 1997 9 /id} {Xu, 2002 121 /id} {Guler, 2002 119 /id}.

In stark contrast to the TRP channels, our data indicated that I_{AT} showed no Ca^{2+} permeability. TRP channels, including the temperature-activated family members, show very high Ca^{2+} permeability {Caterina, 1997 9 /id} {McKemy, 2002 122 /id} {Xu, 2002 121 /id} {Guler, 2002 119 /id}. We believe that because a snake's body temperature is often above the threshold of I_{AT} , the current would be active a great deal of time and high Ca^{2+} permeability could result and Ca^{2+} induced toxicity like that found for TRPV1 {Jordt, 2000 11 /id}. This does not completely rule out a role for a TRP homology in the generation of I_{AT} in snakes as point mutants of TRPV1 have been shown to have altered Ca^{2+} permeability {Welch, 2000 8 /id}. It is also possible that the temperature sensitivity of TG neurons is not due to single temperature-sensitive ion channels mediating I_{AT} but that there may be cells that express a population of temperature-dependent ion channels that confer temperature-gated behaviors on these cells, as has been seen with cold sensitive neurons from the mouse trigeminal ganglion {Viana, 2002 132 /id}.

The transient cooling-sensitive current (I_{coolAT}) could enhance the sensitivity of thermoreceptors by adding a thermal "edge detection" function to the pit. Presently, there are no literature description of thermosensitive neurons that show currents with similar kinetic and temperature dependence. This current will be the focus of future study.

Our investigations suggest that thermosensation at the pit organ may in part be mediated by I_{AT} , but the behavioral data suggest that the cellular and molecular entities that mediate these processes may be more complex. Thermosensation is probably a complex integrated product of multiple temperature-sensitive currents, possessing unique temperature activation profiles and activation kinetics. The currents we have recorded in these TG neurons may represent only part of the complete array of thermosensitive currents in the pit organ. Our continued investigations will focus on elucidating details such as sensitivity and response time of I_{AT} and I_{coolAT} to allow us to further characterize the contribution of these currents to highly-sensitive thermodetection in snakes.

1.6 References

1. Adams DJ, Smith SJ and Thompson SH. Ionic currents in molluscan soma. *Annu Rev Neurosci* 3: 141-167, 1980.
2. Askwith CC, Benson CJ, Welsh MJ and Snyder PM. DEG/ENaC ion channels involved in sensory transduction are modulated by cold temperature. *PNAS* 98: 6459-6463, 2001.
3. Bullock TH and Diecke F.P.J. Properties of an infrared receptor. *Journal of Physiology* 134: 47-87, 1956.

4. Bullock TH and Fox W. The anatomy of the infrared sense organ in the facial pit of pit vipers. *Q J Microscop Sci* 98: 219-234, 1957.
5. Burgoon PW and Boulant JA. Temperature-sensitive properties of rat suprachiasmatic nucleus neurons. *Am J Physiol Regul Integr Comp Physiol* 281: R706-R715, 2001.
6. Caterina MJ, Leffler A, Malmberg AB, Martin WJ, Trafton J, Petersen-Zeitz KR, Koltzenburg M, Basbaum AI and Julius D. Impaired nociception and pain sensation in mice lacking the capsaicin receptor. *Science* 2000 Apr 14;288 (5464):306 -13 288: 306-313, 2000.
7. Caterina MJ, Schumacher MA, Tominaga M, Rosen TA, Levine JD and Julius D. The capsaicin receptor: a heat-activated ion channel in the pain pathway. *Nature* 389: 816-824, 1997.
8. Cesare P and McNaughton P. A novel heat-activated current in nociceptive neurons and its sensitization by bradykinin. *Proc Natl Acad Sci U S A* 93: 15435-15439, 1996.
9. de Cock BT, Terashima S and Goris RC. Crotaline pit organs analyzed as warm receptors. *Cell Mol Neurobiol* 1: 69-85, 1981.
10. Doiron B, Noonan L, Lemon N and Turner RW. Persistent Na⁺ Current Modifies Burst Discharge By Regulating Conditional Backpropagation of Dendritic Spikes. *J Neurophysiol* 89: 324-337, 2003.
11. Goldenberg SS and De Boni U. Pure population of viable neurons from rabbit dorsal root ganglia, using gradients of Percoll. *J Neurobiol* 14: 195-206, 1983.
12. Goris R, Nakano M, Atobe Y, Kadota T, Funakoshi K, Hisajima T and Kishida R. Nervous control of blood flow microkinetics in the infrared organs of pit vipers. *Auton Neurosci* 84: 98-106, 2000.
13. Guler AD, Lee H, Iida T, Shimizu I, Tominaga M and Caterina M. Heat-evoked activation of the ion channel, TRPV4. *J Neurosci* 2002 Aug 1;22 (15):6408 -14 22: 6408-6414, 2002.
14. Hamill OP, Marty A, Neher E, Sakmann B and Sigworth FJ. Improved patch-clamp techniques for high-resolution current recording from cells and cell-free membrane patches. *Pflugers Arch* 391: 85-100, 1981.
15. Hellon RF and Taylor DC. An analysis of a thermal afferent pathway in the rat. *J Physiol* 326: 319-328, 1982.
16. Hille B. *Ion channels of excitable membranes*. Sunderland, Mass.: Sinauer, 2001.

17. JONES BS, LYNN WF and Stone MO. Thermal Modeling of Snake Infrared Reception: Evidence for Limited Detection Range. *Journal of Theoretical Biology* 209: 201-211, 2001.
18. Jordt SE and Julius D. Molecular basis for species-specific sensitivity to "hot" chili peppers. *Cell* 2002 Feb 8 ;108 (3):421 -30 108: 421-430, 2002.
19. Jordt SE, Tominaga M and Julius D. Acid potentiation of the capsaicin receptor determined by a key extracellular site. *Proc Natl Acad Sci U S A* 97: 8134-8139, 2000.
20. Jung J, Hwang SW, Kwak J, Lee SY, Kang CJ, Kim WB, Kim D and Oh U. Capsaicin binds to the intracellular domain of the capsaicin-activated ion channel. *J Neurosci* 19: 529-538, 1999.
21. Kuffler DP, Lyfenko A, Vyklicky L and Vlachova V. Cellular Mechanisms of Nociception in the Frog. *J Neurophysiol* 88: 1843-1850, 2002.
22. Lewis CA. Ion-concentration dependence of the reversal potential and the single channel conductance of ion channels at the frog neuromuscular junction. *J Physiol* 286: 417-445, 1979.
23. Liu L and Simon SA. Capsaicin, acid and heat-evoked currents in rat trigeminal ganglion neurons: relationship to functional VR1 receptors. *Physiol Behav* 69: 363-378, 2000.
24. Lynn B and Carpenter SE. Primary afferent units from the hairy skin of the rat hind limb. *Brain Res* 238: 29-43, 1982.
25. McKemy DD, Neuhausser WM and Julius D. Identification of a cold receptor reveals a general role for TRP channels in thermosensation. *Nature* 2002 Mar 7 ;416 (6876):52 -8 416: 52-58, 2002.
26. Moiseenkova VY, Bell B, Motamedi M, Wozniak E and Christensen BN. Wide-Band Spectral Tuning of Heat Receptors in the Pit Organ of the Copperhead Snake (Crotalinae). *Am J Physiol Regul Integr Comp Physiol* 2002 Nov 14; .: 2002.
27. Nagy I and Rang HP. Similarities and differences between the responses of rat sensory neurons to noxious heat and capsaicin. *J Neurosci* 19: 10647-10655, 1999.
28. Newman EA and Hartline PH. Integration of visual and infrared information in bimodal neurons in the rattlesnake optic tectum. *Science* 213: 789-791, 1981.
29. Noble GK and Schmidt A. The structure and function of facial and labial pits of snakes. *Proc Am Philos Soc* 77: 263-288, 1937.

30. Pappas, T. C., Motamedi, M., and Christensen, B. N. Temperature-responsive neurons from pit viper infrared receptors. 2002 Abstract Viewer/Itinerary Planner. Washington DC: Society for Neuroscience . 2002.
31. Reichling DB and Levine JD. Heat transduction in rat sensory neurons by calcium-dependent activation of a cation channel. *Proc Natl Acad Sci U S A* 94: 7006-7011, 1997.
32. Savidge JR, Ranasinghe SP and Rang HP. Comparison of intracellular calcium signals evoked by heat and capsaicin in cultured rat dorsal root ganglion neurons and in a cell line expressing the rat vanilloid receptor, VR1. *Neuroscience* 2001 ;102 (1):177 -84 102: 177-184, 2001.
33. Terashima S and Liang YF. Temperature neurons in the crotaline trigeminal ganglia. *J Neurophysiol* 22: 623-634, 1991.
34. Terashima SI, Goris RC and Katsuki Y. Generator potential of crotaline snake infrared receptor. *J Neurophysiol* 31: 682-688, 1968.
35. Viana F, de la PE and Belmonte C. Specificity of cold thermotransduction is determined by differential ionic channel expression. *Nat Neurosci* 2002 Mar ;5(3):254 -60 5: 254-260, 2002.
36. Vyklicky L, Vlachova V, Vitaskova Z, Dittert I, Kabat M and Orkand RK. Temperature coefficient of membrane currents induced by noxious heat in sensory neurones in the rat. *J Physiol* 517 (Pt 1): 181-192, 1999.
37. Welch JM, Simon SA and Reinhart PH. The activation mechanism of rat vanilloid receptor 1 by capsaicin involves the pore domain and differs from the activation by either acid or heat. *Proc Natl Acad Sci U S A* 97: 13889-13894, 2000.
38. Wills CA and Beaupre SJ. An application of randomization for detecting evidence of thermoregulation in timber rattlesnakes (*Crotalus horridus*) from northwest Arkansas. *Physiol Biochem Zool* 2000 May -Jun ;73 (3):325 -34 73: 325-334, 2000.
39. Xu H, Ramsey IS, Kotecha SA, Moran MM, Chong JA, Lawson D, Ge P, Lilly J, Silos-Santiago I, Xie Y, DiStefano PS, Curtis R and Clapham DE. TRPV3 is a calcium-permeable temperature-sensitive cation channel. *Nature* 2002 Jul 11;418 (6894):181 -6 418: 181-186, 2002.
40. Zar JH. *Biostatistical analysis*. Englewood Cliffs, NJ: 1984.
41. Zhou Z and Neher E. Mobile and immobile calcium buffers in bovine adrenal chromaffin cells. *J Physiol* 469: 245-273, 1993.

2. Design and Testing of a Rapid Focal Hydronic Stimulator for examining electrophysiological responses of thermosensory cells.

2.1 Introduction

The molecular basis of thermal sensitivity is important for clinical science and basic research. The importance of fever in immune response and the involvement of cloned thermal receptors in mechanisms of thermoreception indicate the clinical relevance. The existence of mechanisms to regulate body temperature in homeotherms and the fact that animals will move towards favorable temperature environments demonstrates the fundamental importance of temperature recognition in biology.

The recent cloning of the hot cold receptors sheds light on the molecular basis of thermal transduction, but critical questions remain. On a cellular level, these include characterizing the response of different neurons to temperature changes. On a molecular level, these include identifying other thermal receptor genes. On a biophysical level, these include elucidating the biophysical basis for the response to temperature, an effort that will likely employ a variety of techniques to monitor conformational changes and ionic currents during exposure of preparations to temperature changes.

A technical impediment to further progress in understanding thermal sensitivity is the lack of appropriate devices for generating rapid temperature responses. A variety of devices are commercially available for controlling temperatures of neurons during electrophysiological recording. These devices rely on feedback controllers and resistive heating elements to warm solutions to physiological temperatures or upon feedback controllers and thermoelectric devices to achieve desired warming and cooling. The primary purpose of these devices is to investigate the temperature dependence of a physiological phenomenon or to maintain a preparation at a temperature suitable for optimal viability. Although capable of generating slow temperature changes, these devices are not designed or optimized for generating rapid temperature changes, these devices are not designed or optimized for generating rapid temperature changes required for studying gating of temperature sensitive channels.

Investigators that study thermal responses to temperature general often rely on devices constructed or modified in their own laboratories to achieve this objective. These devices exist in two broad categories. The first is the thermoelectric device that is designed to achieve exceptionally rapid responses and the second is the device designed to switch solutions from pre-heated to pre-cooled reservoirs. Each of these categories of devices has disadvantages. With the thermoelectric device the rate of temperature change, on the order of several degrees per second, is slow enough to obscure kinetic components of temperature responses. For instance, with the patch clamp, the rapidity of response for voltage steps with modern amplifiers is sub millisecond. Similarly, investigations of ligand-gated channels employ rapid switching devices to yield sub millisecond devices that are sufficiently fast to reveal kinetic steps. When rapid switching devices are paired with the pre-cooled reservoirs, extremely rapid (sub millisecond) time changes are achieved and this has proven helpful in kinetic studies. However, these systems suffer from two defects. The distance of the reservoir from the output of the system causes heat changes as solutions travel. Also, if the output of the system is through a focal application device, it is difficult to determine the precise temperature of the output. Thus, the systems can be used to elicit very rapid temperature responses, but at a significant cost in precision and accuracy. Also, these systems require the purchase of separate components at significant cost to the investigator.

The device described in this application is designed to combine the best features of the thermoelectric cooling systems and the rapid switching systems. The device uses thermoelectric controlled cooling/heating reservoirs that are positioned near the output of the focal application system. This proximity minimizes heat loss during movement of liquids to the output. Valve-based switching devices designed by ALA Scientific achieve switching times (10-90% ramps) of less than

two milliseconds, a time that is clearly within ALA's manufacturing capabilities and superior to that available from commercial devices.

2.2 Preliminary Work

In this project we chose to work with ALA Scientific Instruments, under the direction of Alan Kriegstein. In 1993 ALA introduced the DAD-12 Computer Controlled Drug Application Device. This system utilized a proprietary Micromanifold® to focally apply drugs to individual cells under electrophysiological study such as patch clamp. This system was shown to switch solutions at the cellular level in 10-15 msec. Since the DAD's introduction, they have developed other valve based solution exchange systems, mostly incorporating their Micromanifold design, though in several different iterations to broaden the types of experiments the systems can be utilized in. The central creed of development of this product line was/is to provide high-speed solution exchange systems with stationary focal applicators, relying on high-speed valves and fluid dynamics to gain switching speed rather than mechanically moving small tubes back and forth in close proximity to the cell under study. The valve-based systems, in combination with the Micromanifolds®, provide high-speed solution exchange while helping preserve samples by not requiring drugs to flow to the cell bath continuously as stepper systems often do.

In 1997 ALA began to produce an add-on to the DAD and other perfusion systems that would allow the drug solution applied to a cell to enter the cell bath at a specific temperature. This device was/is called the PTR-2000. This device uses a water jacket to keep the temperature of all 12-output tubes of a DAD at constant temperature, be it room, or 37°C or higher. Once we knew we could hold the temperature of the perfusion system at a specific level, and then we reasoned that if we separated the tubes, we theoretically could hold each tube at a different temperature. Just as with a drug application, each solution at different temperature should strike the cell under study in the same rapid fashion.

2.3 Design and Methods

Our prototype device has four channels. Four reservoirs hold up to 5ml of fluid. Each of those reservoirs feed a valve. The valves are wired to a controller for activation via computer or manually. After the fluid passes the valve, it flows to a reservoir that is mounted on what we call the front end (Figure 7). This reservoir is of small proportions and is designed to hold only a fraction of a milliliter of fluid. This tiny reservoir (mini-reservoir) is attached to a thermoelectric device. All four channels are assembled likewise. The four thermoelectrics are mounted to a cube of aluminum that is precisely machined and acts as a heat sink for the four thermoelectrics. The heat sink is plumbed so that cooling water can pass through it to liberate the heat of the thermoelectrics. The cooling system will be designed to give vibration free operation so as not to interfere with electrophysiological recordings.

A controller powers each of the thermoelectric devices. A thermal sensor is placed in the mini-reservoirs to provide feedback to the controller so that it can maintain the temperature accurate to within 0.1°C. For phase one, we will utilize off-the-shelf controller technology for this part of the set-up. In this case, two, two channel controllers (NPI Instruments)

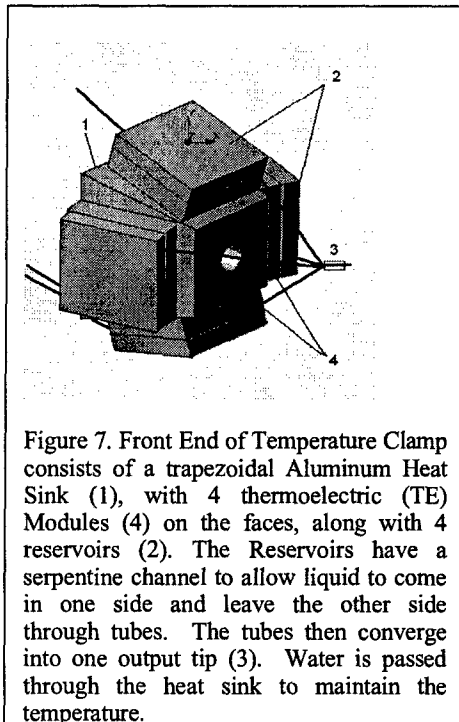


Figure 7. Front End of Temperature Clamp consists of a trapezoidal Aluminum Heat Sink (1), with 4 thermoelectric (TE) Modules (4) on the faces, along with 4 reservoirs (2). The Reservoirs have a serpentine channel to allow liquid to come in one side and leave the other side through tubes. The tubes then converge into one output tip (3). Water is passed through the heat sink to maintain the temperature.

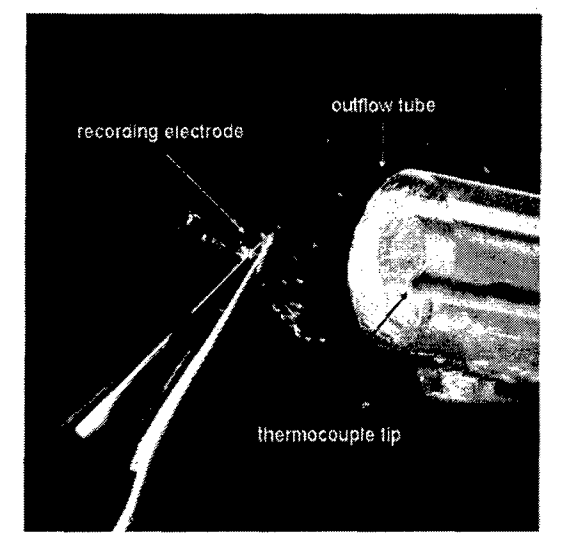


Figure 8. Light micrograph of setup of the focal heating apparatus front end outflow tube, the recording thermocouple and the recording electrode from on the cell in a typical 35 mm diameter recording chamber

be carried by a micromanipulator). When one of the valves opens, air pressure or gravity pushes out the fluid of that channel so that it bathes the target cell(s). Thus the fluid that is emitted delivers the desired temperature to the cell(s) hydraulically. Until the mini reservoir runs out of fluid, the cell(s) are essentially clamped at the temperature of that channel. How long the specific temperature lasts on the cell is a function of how large the mini-reservoir is and the flow rate. These are features that will need to be looked at in this project to determine optimum sizes and flow rates.

2.4 Results

Temperature stimulus characteristics in typical cell culture recording chamber (35 mm diameter dish).

The focal heating apparatus was attached to a three axis micromanipulator and placed in the bath with the fluid stream within 0.2-0.5 mm from the recording thermocouple. We obtained more consistent temperature recordings by running the thermocouple down the fluid ejection tube so that the expose sensing end is just at the tip of the ejection pathway (see Figure 8). Correction for the transit time to the cell can be determined by examining the resistance change at the tip of a cell recording microelectrode.

The relationship of the temperature stimulus characteristic to the fluid ejection pressure, which is proportional to the flow rate, is shown in the Figure 9. The reservoir control valves are controlled with TTL outputs using an ITC 18 digital to analog converter. The valves were manipulated using HEKA Pulse (v. 8.54), which is also used for acquisition of electrophysiology data. Figure 9 shows temperature profiles under different flow rates where the system is changed from room temperature ($22.8 \pm 0.2^\circ\text{C}$) with a 3 s stimulus from the channel at 40°C , followed by a 1.5 s cooling stimulus from a channel at 11°C . Data from an independent experiment is presented in Table 3.

with PID feedback control will be utilized. The controllers will allow us to set the temperature of the mini reservoirs and hold them constant. The controllers can be set manually or using analog inputs that make them compatible with virtually all data acquisition systems for electrophysiology.

The way that the system functions is as follows: Four solutions will be loaded into the four reservoirs of the system. Depending on the experiment, they may be the same solution, or different in each reservoir. The idea is that each solution represents a different temperature. After the solutions are loaded and primed down to the output end, the controllers are set to the desired temperature. Each channel is allowed to come to temperature (5-10mins). The front end, with the Micromanifold® having a tip diameter of $100-200\mu\text{m}$, is pointed at the subject cell(s). (The front end will be small and light enough to

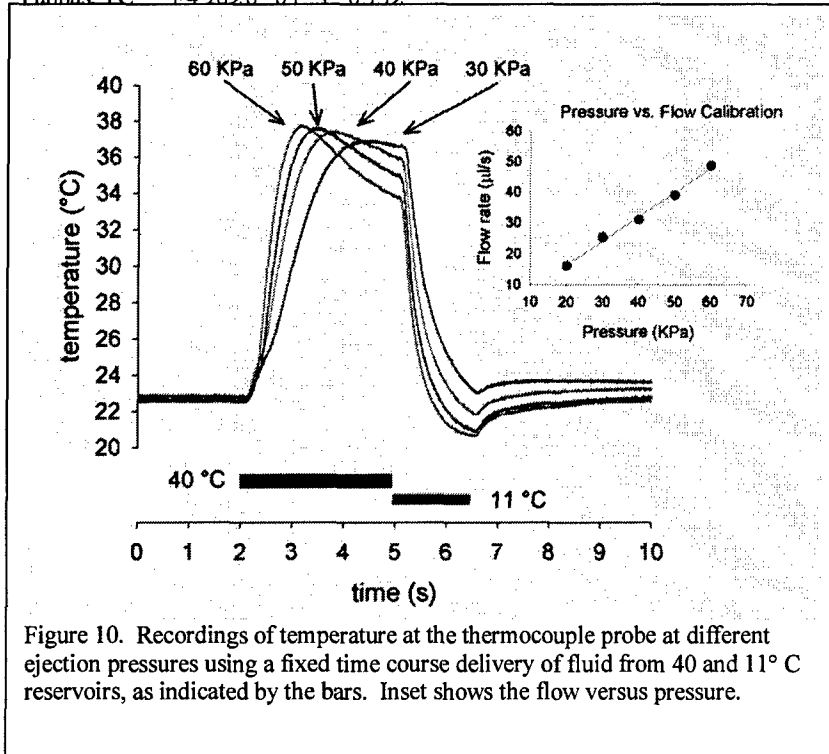


Figure 10. Recordings of temperature at the thermocouple probe at different ejection pressures using a fixed time course delivery of fluid from 40 and 11°C reservoirs, as indicated by the bars. Inset shows the flow versus pressure.

of $0.17 \pm 0.05^\circ\text{C}/\text{s}$. The cells were then cooled with chilled HBS at a rate of $2.0 \pm 1.0^\circ\text{C}/\text{s}$ back to baseline temperature to show reversal of the response.

In the example from three traces shown in the Figure 11, we were able to reach a much higher final temperature. The temperature stimulus protocol is identical to that of figure 10 at 30 KPa. Here we record heating of a 35 mm diameter dish (2-3 mL) from resting temperature of $22.7 \pm 1.7^\circ\text{C}$ to final temperature $40.5 \pm 0.6^\circ\text{C}$. The heating rate (from second 2-3) was $9.5 \pm 0.2^\circ\text{C}/\text{s}$,

while the cooling rate (5.5-6.5s) of $10.8 \pm 0.6^\circ\text{C}/\text{s}$. The temperature loss at holding (4-5s) was $0.6 \pm 0.2^\circ\text{C}/\text{s}$ and represents our most variable and problematic temperature change. This is minimized with lower rate delivery, but at the expense of heating and cooling rates (see figure 10).

We conclude that the focal heating apparatus gives us more rapid and replicable heating and cooling rates and gives us the flexibility to alter the rates by controlling the heating and cooling channels. The apparatus has some problem holding the steady state of the temperature jump, however, probably due to cooling of the element by fluid flow. This is an area of improvement for subsequent design.

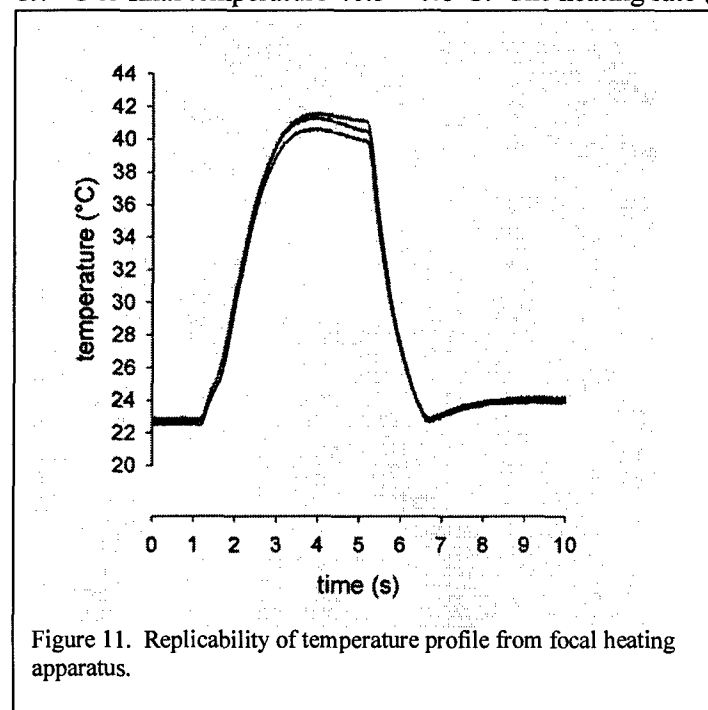


Figure 11. Replicability of temperature profile from focal heating apparatus.

Table 3.

| | 35 KPa | 50 KPa | 70 KPa |
|-------------------------|--------|--------|--------|
| rise time 25-30 °C (ms) | 365 | 239 | 189 |
| heating rate °C/s | 13.7 | 20.9 | 26.4 |
| time for 1 °C jump (ms) | 73 | 48 | 38 |

Temperature response in transfected cells.

TREK-1 is a member of the two-pore domain K⁺ channel family that show temperature sensitivity (8). We transfected a plasmid encoding wild-type murine TREK-1, under the control of the CMV promoter, into COS-7 cells and recorded 24-48 hr after transfection. TREK-1 expressing cells were identified by co-transfection with a GFP expressing plasmid (Invitrogen).

Figure 12 shows temperature response of TREK-1 recorded under current clamp (Fig 12B, D) after heating and cooling (Fig 12A,C) with the apparatus. The heating and cooling profiles of Figure 12 A and C are different from Fig 10 because a larger, insulated thermocouple was used and there was no temperature reversing stimulus at the end of the initial stimulus. The thermal information

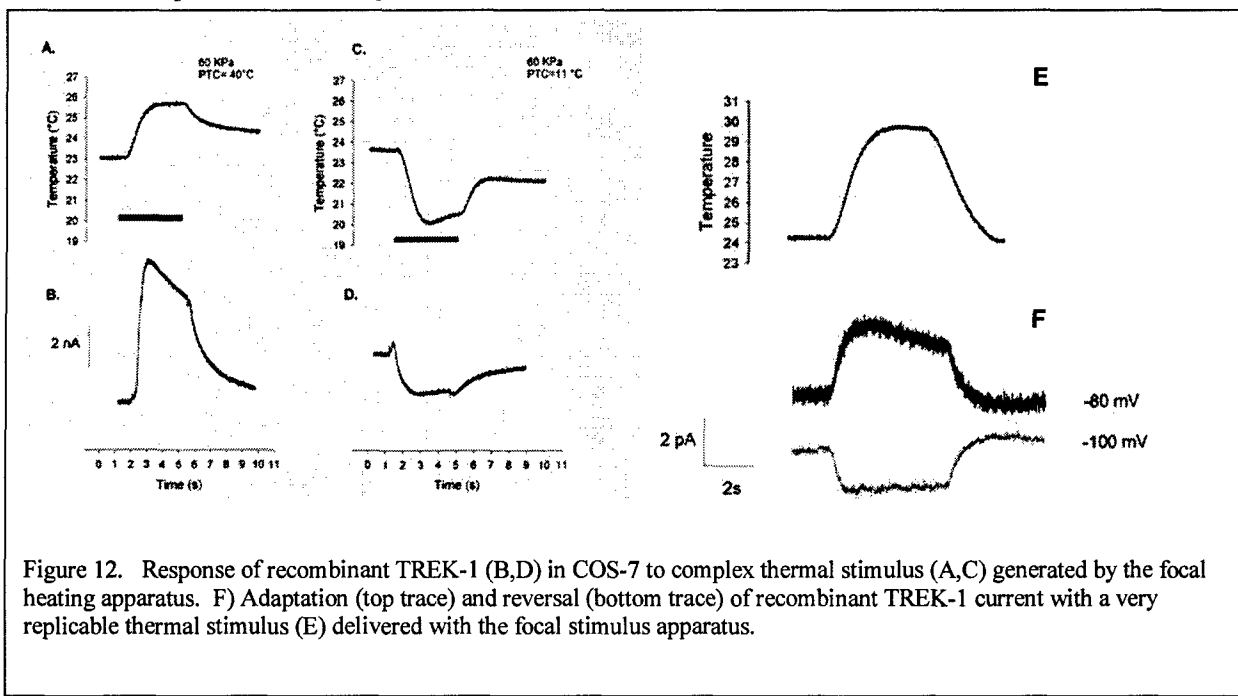


Figure 12. Response of recombinant TREK-1 (B,D) in COS-7 to complex thermal stimulus (A,C) generated by the focal heating apparatus. F) Adaptation (top trace) and reversal (bottom trace) of recombinant TREK-1 current with a very replicable thermal stimulus (E) delivered with the focal stimulus apparatus.

from Figure 12E was recorded with the thermocouple inside the delivery tube, and showed very even heating and cooling ramps with a good steady-state temperature plateau. TREK-1 showed a rapid and adapting response to heating stimulus under all heating conditions (Fig. 12B, F) with a reversal of the current direction at -100 mV. Interestingly, Fig 12B and F show the current rise time faster than the temperature rise time, indicating that the apparatus may not deliver a sufficiently fast stimulus (to this plateau) to obtain ensemble kinetic rates from these currents.

Thermal Stimulation of two unique temperature-responsive currents in dissociated neurons from copperhead (*Agkistrodon contortrix*) trigeminal ganglion.

Pit vipers have highly sensitive thermal receptors that are innervated from the trigeminal ganglion. Our laboratory is the first to have recorded unique, low threshold temperature-sensitive currents from neurons dissociated from this ganglion (9). We are currently using the apparatus to further characterize the kinetics and ion dependence of these current.

Figure 13 shows two unique currents we have consistently identified in TG neurons. The response is to an identical temperature step. I_{AT} is an inward current that matches the temperature step without noticeable desensitization (see fig below). I_{coolA} is a "differential" current that is transient and inward and response only to cooling. Interestingly, our data on I_{coolA} show that it does not have a threshold. It responds to cooling regardless of the initial temperature. This focal heating apparatus will allow us this current in a more detailed fashion. We will be able to examine a broad but precise range of initial temperatures to find a threshold range for gating. We will also be able to change the magnitude and ramp speed of the cooling step to examine how these factors change the current magnitude. The ability to program rapid and complex temperature changes will greatly aid the investigation of this unique current.

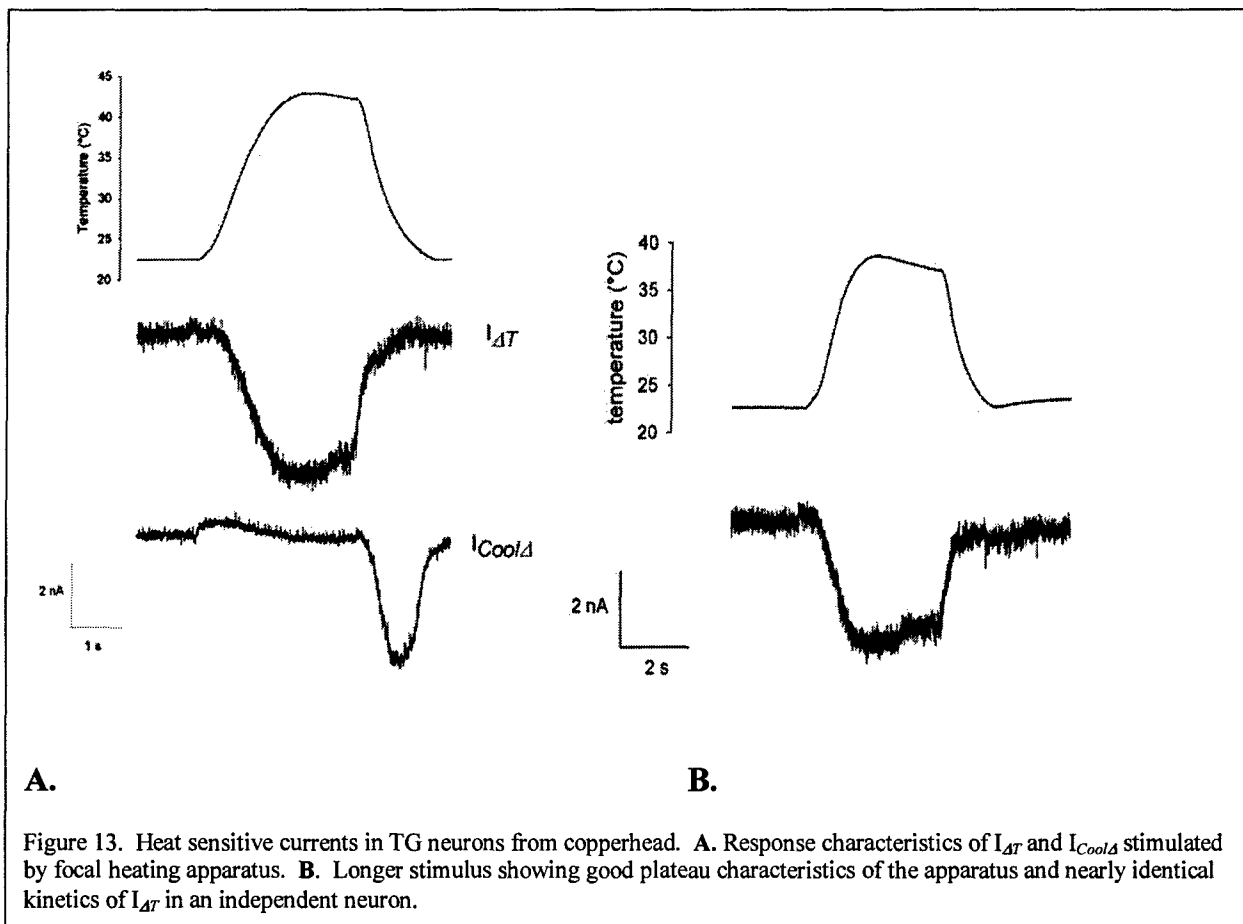


Figure 13. Heat sensitive currents in TG neurons from copperhead. A. Response characteristics of I_{AT} and I_{coolA} stimulated by focal heating apparatus. B. Longer stimulus showing good plateau characteristics of the apparatus and nearly identical kinetics of I_{AT} in an independent neuron.

2.5 General Methods

Culture of Trigeminal Ganglion. Cell bodies that have sensory terminal nerve specializations in the infrared/heat-sensitive pit organ are found in the ganglia of ophthalmic, maxillary, and mandibular branches of the trigeminal nerve (2). Snakes were anesthetized with Isofluorane USP (Abbott Laboratories, North Chicago IL) then decapitated and the head was placed on ice to minimize cell death after decapitation. The TG was located visually, removed, and placed in ice-cold F12:DMEM (Gibco BRL). Cells were dissociated from the ganglia by treatment with collagenase (1 mg/mL, 45 min, 28°C) and trypsin (2.5 mg/mL, 5 min, 22°C) followed by mechanical dissociation with plastic pipettes. The dissociated cell mixture was layered onto 25 % percoll (Sigma Chemical Co, St Louis MO) and centrifuged for 10 min at 500 xg to remove large cell bodies and debris (4). Cells were cultured in F12:DMEM supplemented with 10% fetal bovine serum, 10 U/mL penicillin, 10 µg/mL streptomycin (Gibco BRL) and 2 mM glutamine (Gibco BRL) on 35 mm diameter tissue culture plastic dishes (Falcon). Cells were maintained at 28°C in 7% CO₂/93% air for 16-96 hrs.

COS-7 COS-7 cells were cultured in DMEM supplemented with 10% fetal bovine serum, 10 U/mL penicillin, 10 µg/mL streptomycin (Gibco BRL) and 2 mM glutamine (Gibco BRL) on 35 mm diameter tissue culture plastic dishes (Falcon). Cells were transfected with 0.25 to 0.5 µg/dish plasmid DNA using Lipofectamine (Invitrogen) according to the manufacturer's protocol. Plasmids were a gift from Dr. Steve A.N. Goldstein (Yale University) and coding sequence was transfected into PCMV-Tag4A (Invitrogen) in the laboratory of Dr. Paul Blount (UT Southwestern, Dallas). Cells were maintained at 37°C in 5% CO₂/95% air for 24-48 hrs prior to recording.

Electrophysiology. Recordings from neurons and transfected cells were made in 35 mm diameter dishes on an Olympus IX-71 inverted microscope. Currents were recorded in HEPES-buffered saline (HBS, in mM: NaCl 130, KCl 3.0, CaCl₂ 2.0, MgCl₂ 1.2, HEPES [pH 7.3] 10, glucose 10). Neurons were voltage clamped using single patch electrodes in the whole-cell mode and held at -70 mV using an SEC-05LX amplifier (NPI Electronics GmbH, Tamm, Germany) interfaced to a computer using an ITC-18 interface (Instrutech Corp.). Patch pipettes were made from 1.5 mm OD 8515 glass (Warner Instruments) and pulled to a resistance of 2-5 MΩ using a Sutter Instruments P 87 puller. Patch electrode solutions contained 140 mM K-gluconate, 2 mM MgCl₂, 2 mM 1,2-bis(2-aminophenoxy) ethane- N,N,N',N'-tetraacetic acid (BAPTA), 0.2 mM CaCl₂, and 1 mM HEPES with a pH 7.4. K-gluconate was substituted with KCl in some experiments. Voltage clamp protocols were controlled using HEKA Pulse (v. 8.54, HEKA Instruments Inc.). Temperature was recorded using a 40 ga T-type (copper-constantan) polyurethane insulated thermocouple (model T088G, Physitemp) interfaced with a Bailey Instruments BAT-9 temperature recorder.

3. Molecular Engineering of Thermosensitive Proteins

3.1 Introduction

Electrophysiological investigation of pit viper trigeminal neurons revealed multiple temperature sensitive currents but did not yield information on the molecular identity of proteins that may mediate these responses. The lack of a Ca²⁺ conductance makes it unlikely that the proteins mediating these responses are anything like the cloned mammalian thermoreceptors of the TRPV family (5) or from other known thermosensitive proteins (1; 8). Additionally, our proposed proteomic study, which was designed to find candidate thermosensitive proteins, was actually completed by another group during the course of our study (13). The findings in this publication actually illustrated the weaknesses of the proposed proteomic approach. Given the nature of the tissue in the pit organ, mostly nerve endings, and the microscopy finding of numerous mitochondria in this location it was not surprising that this study identified mostly mitochondrial proteins. Protein

mapping and identification studies are biased towards high abundance proteins (6), and there is no indication that thermosensory proteins are abundant.

We took two alternative approaches to finding thermosensory proteins with the sensitivity characterized at the pit organ. The first was to search the transcripts from snake trigeminal ganglion for homologues of characterized mammalian thermoreceptive proteins. The second was to use combinatoric protein engineering to manufacture thermosensitivity into ion channels. Neither of these approaches yielded results, mostly from technical difficulties, but the studies are summarized below.

3.2 Low Stringency PCR Identification of TRPV1 Homologues from Pit Viper Trigeminal Ganglion.

Methods and Results

Low stringency hybridization of nucleic acid probes has been used extensively to probe for gene homology. Several PCR methodologies exist to take advantage of this feature. We used both low hybridization temperatures, which favors lower specificity hybridization of the amplification probes, and "touchdown" PCR, which has increase hybridization temperatures as the amplification continues, favoring the most specific product. Total RNA was isolated from Western Diamondback Rattlesnake (*C. atrox*) trigeminal ganglion, optic tectum and telencephalon using RNAqueous 4-PCR kit (Ambion, Austin TX). Typical RNA yield and purity for 4 ganglia or one each optic tectum and telencephalon are presented in Table 4.

Table 4.

| Sample | 260 | 280 | 260/280 | Concentration (ug/mL) | total (ng) |
|---------------|--------|--------|----------|-----------------------|------------|
| Ganglion | 0.0132 | 0.0076 | 1.736842 | 5.28 | 369.6 |
| Optic Tectum | 0.1476 | 0.0733 | 2.013643 | 59.04 | 4132.8 |
| Telencephalon | 0.2164 | 0.1066 | 2.030019 | 86.56 | 6059.2 |

We used 1-2 µg of the total RNA in our RT reaction. We used the Superscript II reverse transcriptase system (Invitrogen) and primed the total RNA from oligo dT. For the PCR reactions, 1 µl of the reverse transcription reaction was used. For low stringency PCR we employed 2-cycle PCR on a gradient thermocycler profiles using 95 °C (15 s) denaturation and from 50-60°C (30s) hybridization/extension for 35 cycles. For "touchdown" PCR, a 3 cycle protocol was used where the denaturation was done at 95 °C (15 s), the annealing was started initially at 60 °C but was decreased each subsequent cycle so that it was 50°C after 30 cycles. Extension was at 72°C for 30 s. Each of these PCR protocols favors the amplification of less stringent hybridizing sequences. The primer sets were predicted from the rat TRPV1 sequence published on NCBI (NM_031982). The 5'-3' sequences are VR1-1334 GAACCGACTCCTACAGGACAA, VR1-2147 AATCTTCTTGACGGTCTCACCA. This yielded a 813 bp product from a plasmid containing the coding sequence for the rat TRPV1 (not shown). Other primer pairs from rat TRPV1 or TREK1 never yielded a positive result and are omitted.

Representative results from these PCR reactions are shown in Figure 14. These results generally indicate that it was difficult to obtain gene products from PCR. Controls using the rat TRPV1 plasmid showed positive products. The products presented in Figure 14A were cloned into pcDNA3.1/V5-His TOPO using topoisomerase cloning (Invitrogen). These products were actually amplicon contamination products and, when sequenced, yielded 100% homology with the rat

TRPV1. Upon subsequent iterations when the TRPV1 contamination was overcome we were able to obtain a unique snake-derived sequence from the PCR, but TOPO cloning and subsequent analysis revealed no homology to any known sequences. Cloning of the full length sequence was not pursued.

As an alternative approach to PCR cloning, we attempted to manufacture a cDNA library from snake trigeminal ganglia. *C. atrox* was used as it was larger and less expensive. Trigeminal ganglia were removed from CO₂- anesthetized snakes. About 50 snakes were used to obtain about 200 µg of total RNA. The cDNA library was manufactured using the ZAP cDNA synthesis and ZAP cDNA library kits from Stratagene (La Jolla, CA). The library synthesis was done in the laboratory of Dr. Helen Hellmich at UTMB. There was, unfortunately, a technical problem in the packaging of the cDNA pieces into the library, which we now believe to be a failure of the "helper phage" and the yield of the library was very low. We estimate only 10⁵ sequences were packaged, rather than the 10⁹ needed for good screening. Regardless of these problems, we sent the library to the laboratory of Dr. David Julius (UCSF) for screening by Dr. Sven-Eric Jordt. He was unable to find sequences with any homologies to TRPV1, TRPV2 or TRPV3, owing to the low titer of the library. We did not have adequate resources to obtain new snakes for a replicate of this procedure.

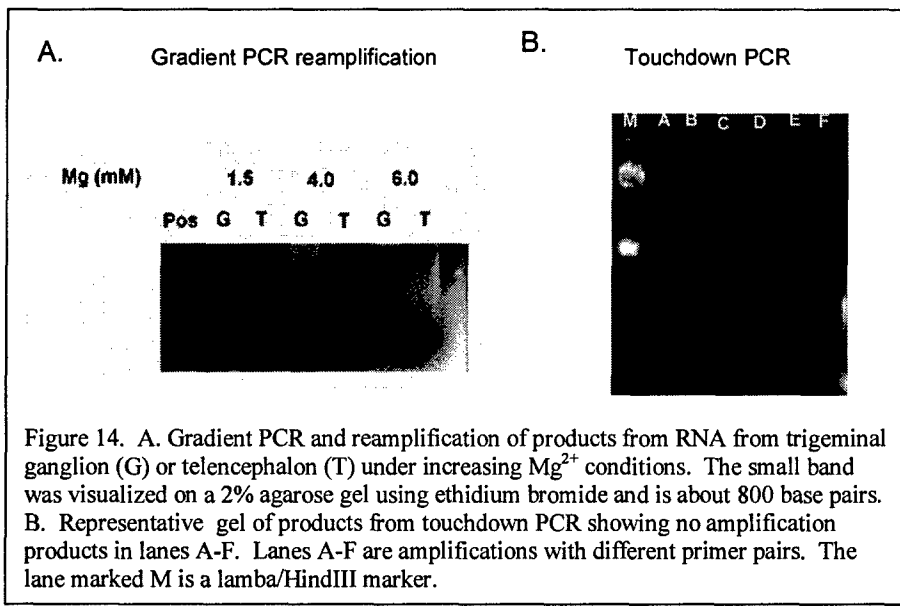


Figure 14. A. Gradient PCR and reamplification of products from RNA from trigeminal ganglion (G) or telencephalon (T) under increasing Mg²⁺ conditions. The small band was visualized on a 2% agarose gel using ethidium bromide and is about 800 base pairs. B. Representative gel of products from touchdown PCR showing no amplification products in lanes A-F. Lanes A-F are amplifications with different primer pairs. The lane marked M is a lambda/HindIII marker.

3.3 Directed Evolution of TRPV1 Protein.

Our alternative approach to engineering high temperature sensitivity into ion channels was to use protein engineering techniques to alter the thermosensitivity of known ion channels. We believed that the best candidate molecules for

engineering would be previously cloned ion channels with known thermosensitivity, TRPV1 and TREK1. Of these two, TRPV1 was selected as the best because a) it is a Ca²⁺ channel (3) so interesting mutants could be expression-selected by monitoring heat-induced Ca²⁺ influx and b) mutations that change the thermosensitivity of the channel have already been identified (7). Because there was no known 3D structure of TRPV1 nor predictable alteration that would change thermosensitivity we decided to alter portions of the channel combinatorically and select for mutants that show our desired characteristics. This is called directed evolution (11).

3.4 Methods and Results

The methods we chose to use take advantage of the infidelity of base incorporation of *Taq* polymerase under certain ionic conditions, where numerous cycles of amplification can generate sequence diversity (10). We chose to use a process called staggered extension process (StEP (12)) to generate sequence diversity in TRPV1. The process and representative results are presented in

Figures 15 and 16 below. In these figure we demonstrate that StEP PCR procedure was used to generate full length products using a TRPV1 (VR1) template, as evidenced in Figure 15. Each lane represents a separate reaction, and multiple reactions were run so as to generate sufficient product for subcloning into the mammalian expression vector pTracerTM-CMV2 (Invitrogen) for subsequent expression screening. The vector has a multiple cloning site for insertion of the product digested with the restriction enzymes Kpn I and Xba I, allowing for a directional insertion of the StEP product into the expression vector (Figure 16A). This vector has a GFP indicator protein that glows green under proper illumination and indicates for us which cells are expressing the protein. The GFP expression is initiated by an internal ribosome entry site, so it is a separate protein.

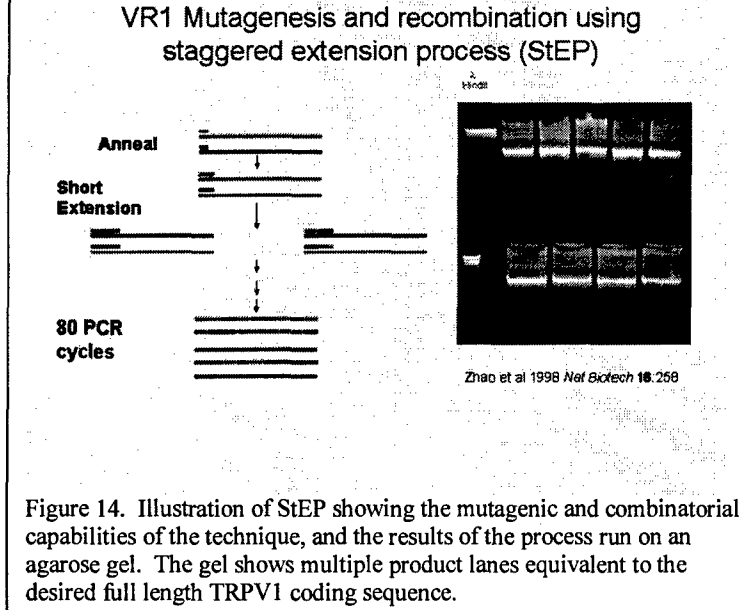


Figure 14. Illustration of StEP showing the mutagenic and combinatorial capabilities of the technique, and the results of the process run on an agarose gel. The gel shows multiple product lanes equivalent to the desired full length TRPV1 coding sequence.

although it is from the same transcript as the TRPV1-StEP product, it is a separate protein.

This product was then amplified using typical recombinant DNA techniques, and the vector was purified for transfection into mammalian cells. A diagnostic digest is presented in Figure 16B and shows that the TRPV1 product was inserted into the vector. The product was then transfected into HEK293 cells using lipid mediated transfection (Lipofectamine, Invitrogen) and the presence of GFP was monitored optically (Figure 16C). At this point, the project was terminated because the technical personnel had taken another position. No further work has been done on the project, although at least one StEP library from TRPV1 exists and has been subcloned into the expression vector. It is not clear what the sequence diversity in the StEP library is at this point, and diagnostics for sequence diversity would need to be performed on this library prior to selection.

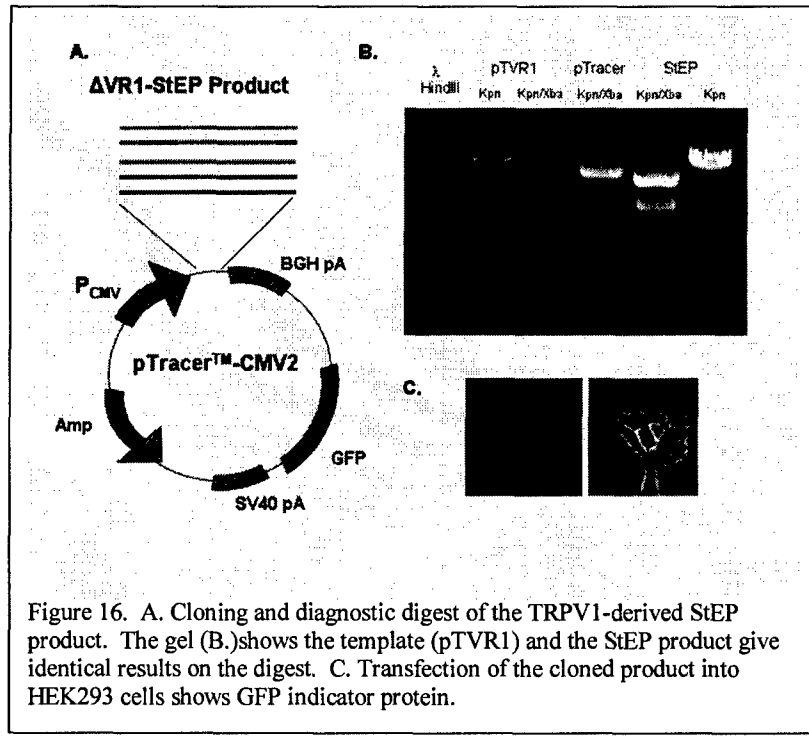


Figure 16. A. Cloning and diagnostic digest of the TRPV1-derived StEP product. The gel (B.) shows the template (pTVR1) and the StEP product give identical results on the digest. C. Transfection of the cloned product into HEK293 cells shows GFP indicator protein.

3.5 References

1. **Askwith CC, Benson CJ, Welsh MJ and Snyder PM.** DEG/ENaC ion channels involved in sensory transduction are modulated by cold temperature. *PNAS* 98: 6459-6463, 2001.
2. **Bullock TH and Fox W.** The anatomy of the infrared sense organ in the facial pit of pit vipers. *Q J Microscop Sci* 98: 219-234, 1957.
3. **Caterina MJ, Schumacher MA, Tominaga M, Rosen TA, Levine JD and Julius D.** The capsaicin receptor: a heat-activated ion channel in the pain pathway. *Nature* 389: 816-824, 1997.
4. **Goldenberg SS and De Boni U.** Pure population of viable neurons from rabbit dorsal root ganglia, using gradients of Percoll. *J Neurobiol* 14: 195-206, 1983.
5. **Guler AD, Lee H, Iida T, Shimizu I, Tominaga M and Caterina M.** Heat-evoked activation of the ion channel, TRPV4. *J Neurosci* 2002 Aug 1;22 (15):6408 -14 22: 6408-6414, 2002.
6. **Jain KK.** Application of laser capture microdissection to proteomics. *Methods Enzymol* 356: 157-167, 2002.
7. **Jordt SE, Tominaga M and Julius D.** Acid potentiation of the capsaicin receptor determined by a key extracellular site. *Proc Natl Acad Sci USA* 97: 8134-8139, 2000.
8. **Maingret F, Lauritzen I, Patel AJ, Heurteaux C, Reyes R, Lesage F, Lazdunski M and Honore E.** TREK-1 is a heat-activated background K(+) channel. *EMBO J* 19: 2483-2491, 2000.
9. **Pappas TC, Motamedi M and Christensen BN.** Unique temperature-activated neurons from pit viper thermosensors. *American Journal of Physiology-Cell Physiology* 287: C1219-C1228, 2004.
10. **Stemmer WP.** DNA shuffling by random fragmentation and reassembly: in vitro recombination for molecular evolution. *Proc Natl Acad Sci USA* 91: 10747-10751, 1994.
11. **Stemmer WP.** Rapid evolution of a protein in vitro by DNA shuffling. *Nature* 370: 389-391, 1994.
12. **Zhao H, Giver L, Shao Z, Affholter JA and Arnold FH.** Molecular evolution by staggered extension process (StEP) in vitro recombination. *Nat Biotechnol* 16: 258-261, 1998.

13. **Zischka H, Keller H, Kellermann J, Eckerskorn C and Schuster SC.** Proteome analysis of the thermoreceptive pit membrane of the western diamondback rattlesnake *Crotalus atrox*. *Proteomics* 3: 78-86, 2003.